Desalination and Water Treatment 320 (2024) 100758

Contents lists available at ScienceDirect

Desalination and Water Treatment

journal homepage: www.sciencedirect.com/journal/desalination-and-water-treatment/

Carbon as a multifunctional material in supporting adsorption performance for water treatment: Science mapping and review

Heryanto Heryanto [a,*,1], Dahlang Tahir [a], Bualkar Abdullah [a], Mustafa Kavgaci [b], Asnan Rinovian [c], Rachid Masrour [d], Venkata Siva Rama Prasad [e], M.I. Sayyed [f]

[a] Department of Physics, Hasanuddin University, Makassar 90245, Indonesia
[b] Department of Opticianry, Kahramanmaras Istiklal University, Kahramanmaras 46080, Turkey
[c] Research Center for Mining Technology, National Research and Innovation Agency (BRIN), Lampung, 35361, Indonesia
[d] Laboratory of Solid Physics, Faculty of Sciences Dhar El Mahraz, Sidi Mohamed Ben Abdellah University, BP 1796 Fez, Morocco
[e] Department of Civil Engineering, Malla Reddy Engineering College, Secunderabad 500100, India
[f] Department of Physics, Faculty of Science, Isra University, Amman 11120, Jordan

ARTICLE INFO

Keywords:
Activated carbon
Surface area
Adsorbents
Bibliometric analysis

ABSTRACT

This review article aims to present the evaluation of research progress in the field of adsorption, identified based on 35,245 articles from 2003–2023 utilizing the Scopus database via bibliometric analysis to determine the countries, most active journals, and keyword relationships that indicate knowledge-exchange and collaboration pathways. The role of density functional theory and the second-order (Y) of adsorption modelling such as response surface methodology and artificial neural networks from input items (adsorbent concentration x_i, adsorbent type x_{i2}, etc.) has become an option for designing the optimization of specific pollutant degradation as output due to its controllability in optimized experimental conditions for maximum adsorption efficiency. Meanwhile, the development of isotherm models from Freundlich in 1906 to Liu in 2018 shows that adsorption intensity affects the k_f by changing the thermodynamic conditions as a consequence. To summarize, the optimization of adsorption properties through various methods and models has led to significant research on carbon and activated carbon (AC) for water remediation, with a trend towards using AC with semiconductors and exploring multifunctional applications. Additionally, carbon (black, fiber, nanotube form) and AC are discussed as materials that have been employed in the fields of civil engineering, energy storage, biomedicine, and sensors due to their conductivity, specific surface area, and detoxification properties. Finally, this review is beneficial for researchers focused on finding the scientific justification and development of carbon and AC as promising adsorbents.

1. Introduction

The challenge of clean water availability is one that must be addressed immediately since it significantly impacts the health of humans [1,2], as well as environmental sustainability. In terms of developing methods for separation and purification, considerable focus has been placed on the adsorption process as a result of its uncomplicated, cost-effective, and environmentally friendly characteristics [3,4]. In principle, adsorption involves the increased concentration of a substance at the condensed layer–liquid/gas interface resulting from the surface force operation [5]. Carbon and activated carbon (AC) have been widely used as adsorbents with promising performance, and have even been investigated as a capacitor material [6], for renewable energy conversion [7], and as ultra-small nanoparticles [8]. Although the role of carbon is not as significant as AC in its implementation, its presence is widely employed as doping in an effort to improve the properties of the involved semiconductors. This is not separated from the characteristics of a large surface area that favors sufficient pore distribution and the provision of active sites that can act as traps [9]. Based on their source, adsorbents can be categorized into synthetic and natural materials. Clay minerals and biological biomass are presented as natural sources, while nanoparticles and metal ions reported to be utilized as adsorbents are

---

* Corresponding author.
E-mail address: heryanto@science.unhas.ac.id (H. Heryanto).
[1] ORCID: https://orcid.org/0000–0002-7057–7898

https://doi.org/10.1016/j.dwt.2024.100758
Received 25 June 2024; Received in revised form 30 August 2024; Accepted 4 September 2024

included as-synthesized materials [10].

This review article uses the bibliometric analysis method by utilizing the Scopus database to collect data, which will not only provide objective and quantitative information with which to evaluate the reported scientific outputs, impacts, and trends but will also provide an overview of the scientific literature [11], as well as specifying the countries, most active journals, and keyword relationships that indicate the pathways of knowledge exchange and collaboration. Compared to previous related works that only highlighted carbon dots in the adsorption of pharmaceuticals [12], the ability of biochar in phosphate degradation [13], and also extends the scope to include all types of carbon and AC for adsorption purposes. Our results not only support previous findings but also introduce a new dimension to the explanation of how carbons and ACs perform in photocatalysis.

In the bibliometric analysis, 35,245 articles were found to have reported research results corresponding to the keywords ("carbon", "activated carbon", and "adsorption") in the 2003–2023 period. Carbon and AC were chosen because they are recognized as one of the most efficient adsorbents due to their outstanding characteristics, such as a highly developed porous structure, diverse oxygen functional groups, excellent thermal and mechanical stability, high adsorption capacity, and large surface area [14]. However, when the keyword "photocatalyst" was included, the number of articles decreased significantly to 280. This indicates that although several types of adsorbents with various performances have been reported, few articles focused on including in-depth explanations of the physical and chemical phenomena involved in the degradation process. In fact, a discussion of the equilibrium conditions, the adsorption capacity of adsorbents, isotherms, and kinetic processes is vital to achieving optimization so that the applied design can be obtained [15,16].

This review article is organized as follows: In Section 1, we reviewed the basic theory and background relevant to adsorption and adsorbent types such as AC and charcoal. Section 2 describes bibliometric analysis as a method of searching data on the application of AC as an adsorbent. Section 3 discusses various activation methods of carbon and their applications in various research fields. Finally, Section 4 offers conclusions, implications, and recommendations for future research to explore its applications in civil engineering, energy storage, biomedical fields, and electronics. Additionally, artificial neural networks and the response surface methodology present themselves as novel modeling that can optimize the experimental conditions for maximum adsorption efficiency [17]. Indeed, the combined use of both empowers researchers to optimize and develop predictive models [18]. Thus, identifying significant factors and their interactions, as well as developing mathematical models to predict the response, represent important advances in the effort to improve the adsorption process.

1.1. Adsorption

The physicochemical technique that dissolves molecules in water that are chemically and physically bound to the surface of the adsorbent as shown in Fig. 1 is referred to as the adsorption phenomenon. In terms of effectiveness, adsorption technology is the optimum procedure because it contains degradation steps such as dye diffusion/convection, and dye molecules' diffusion (i) via the diffusion boundary layer, (ii) from the surface of the adsorbent material's interior, and (iii) from the surface to the adsorbent material's interior [19,20]. Physisorption is the process of adsorbate attaching to a surface through van der Waals forces that occurs at low temperatures and is influenced by factors such as molecular size and surface area [21]. Chemisorption, on the other hand, involves chemical bonds forming between the adsorbate and adsorbent upon the formation of a single layer and is difficult to reverse. Upon the absorption of light energy, the photocatalyst generates electron-hole pairs [22].

These charge carriers are crucial in terms of promoting photocatalytic reactions, triggering surface diffusion events, and increasing adsorption capacity with the consequence of making the adsorbent better at adsorbing substances. These charge carriers have importance in terms of driving the photocatalytic reaction to trigger surface diffusion events. The movement of adsorbates on the material surface is motivated by surface diffusion, where adsorbates are reactant molecules that have adsorbed onto the catalyst surface [23]. The dye molecule type also determines the success of the adsorption process, which can be in the anionic–cationic range, where these two charge differences affect the hydrophobic and electrostatic interactions, respectively [24]. In addition, in this review, we use the following variables, which will be discussed below in the paper:

Variable information.

Y= the predicted response.

x_i, x_j= the input variables.

k, ε = the number of variables and residual.

β_0, β_i= the constant term and linear coefficient.

β_{ij}, β_{ii}= the interaction and quadratic term coefficient.

q= the amount of adsorbate adsorbed/mass of adsorbent at equilibrium (mg).

$Q_{\max}$= the maximum adsorption capacity for monolayer coverage.

K_L, K_F= the Langmuir and Freundlich constants related to the adsorption energy.

$[A]$, $[S]$, $[A-S]$ = the concentration of adsorbate, surface, and the reaction product.

q_e, $q_{\max}$ = the fraction of the filled sites at equilibrium, and the maximum capacity of adsorption (mg/g).

C_e= the adsorbates' equilibrium concentration (mg/L).

k_L, R_L= the equilibrium constant and separation factor for the Langmuir model.

k_1, k_2= the rate constant for adsorption and desorption.

C_0= the adsorbate initial concentration.

k_F= the equilibrium constant for the Freundlich model.

K_T, b, T= the Temkin isotherm, Temkin constant, and absolute temperature.

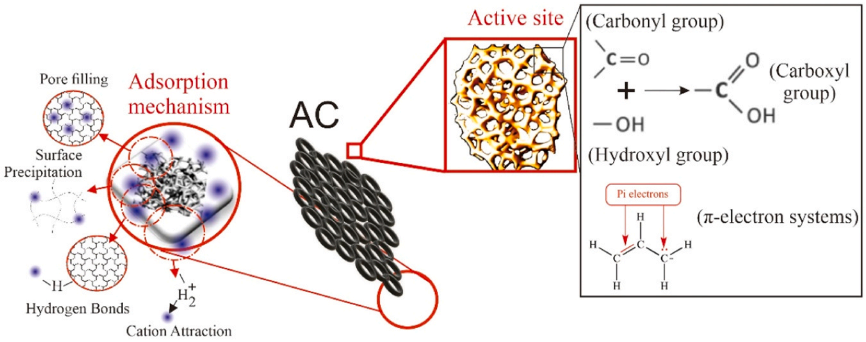

Fig. 1. The adsorption mechanism on the surface of AC.

$1^{1/n}$, R= the Freundlich exponent and regression.

K_H, n_H= the Halsey isotherm constant, and the parameters of the linearized equation.

K_J, A_{HJ}= the Jovanovich constant (L/g), and the Harkin–Jura constant (L/g).

q_{em}, q_t= the amount of metal adsorbed at equilibrium (mg/g), and time (t).

k_1, K_1= the pseudo constant rate, and the reaction rate.

$q_{\max}$, q_m, K_e= the maximum adsorbate uptake, maximum capacity (mg/g), and Elovich constant.

K_{liu}, n_{liu}= the Liu constant and its exponents' model.

K_{int}, C_{int}= the intra-particle diffusion rate constant (min^{-1}), and its intercept.

1.2. Synthetic and natural adsorbents

Determining the type of adsorbent can be classified based on its origins. Synthetic and natural are the two groups that can be used to separate them as shown in Fig. 2. Natural materials can be represented by microorganisms [25], olive stone, and clays [26], while synthetic materials are represented by metal ion nanoparticles [27]. The classification of natural and synthetic adsorbents will provide an overview of the respective advantages and disadvantages. Natural adsorbent materials are of course renewable, sustainable, and low cost, thus rendering them an environmentally friendly option, but it should be noted that they may have limited stability under certain conditions, especially in harsh environments with extreme pH. Synthetic adsorbent materials have the advantage of specific adsorption properties that are useful for targeting specific pollutants.

Generally, synthetic adsorbents show more consistent performance than natural materials as their properties can be standardized, resulting in more predictable adsorption. Because synthetic adsorbent materials are produced through chemical and physical processes, some may lack biocompatibility, making them less suited for interaction with biological systems. The use of a high concentration of metallic materials is also a residual cause that can be a risk in its application.

Therefore, a solution can be achieved in the form of composite materials in order to avoid the limitations of synthetic and natural materials in their utilization as adsorbents. Combining synthetic and natural materials can be modeled as a composite. Therefore, the presence of composite materials is claimed to overcome the shortcomings of such materials that include slow adsorbents, potential contaminants, and limited biocompatibility. Increased adsorption capacity and selectivity, and improved stability are the targets that can be achieved from the composite process. The CaO/C combination provides an opportunity to increase the adsorption capacity as a result of the natural materials' high surface area with specific functional groups of synthetic materials such as CaO [28]. The formation of specific sites on synthetic materials is enhanced by the surface area of AC, and the binding process of adsorbents through the chemical process by TiO_2 coordination in the chemisorption process, thus customizing adsorbents for specific target molecules by combining different binding mechanisms to increase their effectiveness [29]. To achieve limited biocompatibility, the combination of $Fe_3O_4/AC/TiO_2$ as a nanocatalyst has also been reported in stable degradation and reuse studies [30]. Utilizing the durability of synthetic materials along with the inherent biodegradability of natural materials will increase reuse as the materials have a stable response, with electrostatic adsorption the process responsible for this improvement.

1.3. Activated carbon

On the basis of its unique properties, AC has become an option in air purification, desalination, and the treatment of water and wastewater, as a result of its porous nature with up to 90 % of its surface area [31]. Many functional groups like phenol, carboxyl, and carbonyl have responsibility for the outer surface of carbon to improve its adsorption performance [32], because they act as a molecular binder for pollutants, as shown in Fig. 3.

Carbonyl: In organic terms, carbonyl refers to a carbon atom bonded in duplicate to an oxygen atom (C═O). The carbonyl group has the structure $R - C = O$, where R represents an organic substituent. Carbonyl can occur through oxidation and reduction reactions, which can occur in biological molecules and polymerization processes. The electronegativity difference between carbon and oxygen causes carbonyl (electrophilic) groups to have polar properties that are useful for facilitating nucleophilic sites on adsorbates.

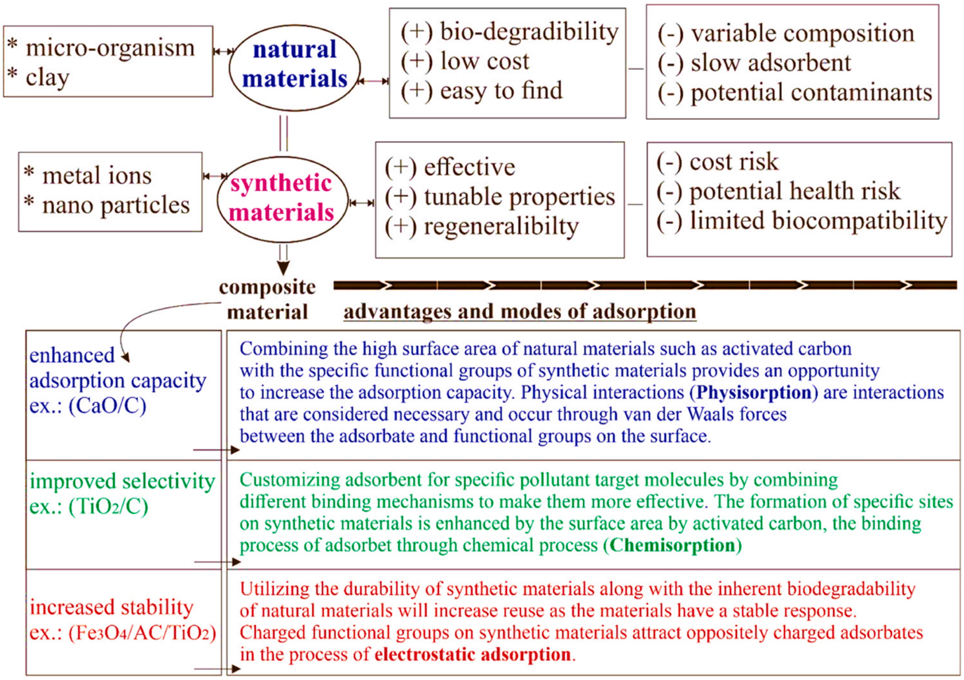

Combining the high surface area of natural materials such as activated carbon with the specific functional groups of synthetic materials provides an opportunity to increase the adsorption capacity. Physical interactions (**Physisorption**) are interactions that are considered necessary and occur through van der Waals forces between the adsorbate and functional groups on the surface.

Customizing adsorbent for specific pollutant target molecules by combining different binding mechanisms to make them more effective. The formation of specific sites on synthetic materials is enhanced by the surface area by activated carbon, the binding process of adsorbet through chemical process (**Chemisorption**)

Utilizing the durability of synthetic materials along with the inherent biodegradability of natural materials will increase reuse as the materials have a stable response. Charged functional groups on synthetic materials attract oppositely charged adsorbates in the process of **electrostatic adsorption**.

Fig. 2. Advantages and limitations of different forms of Synthetic and natural adsorbents.

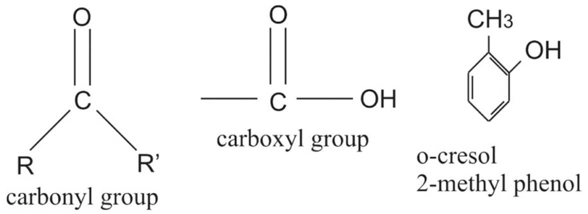

Fig. 3. The chemical structure for the carbonyl group, carboxyl group, and methyl phenol as a binding site.

Carboxyl: Carbon atoms consisting of carbonyl groups ($C = O$) and hydroxyl groups (-OH), which in general can be written as (-COOH), are referred to as carboxyl groups. Carboxyl groups can be formed through oxidation $[R-CH_2-OH \rightarrow R-COOH]$, hydrolysis $[R-CN \rightarrow R-COOH]$, and oxidation $[R-CHO \rightarrow R-COOH]$ reactions. The presence of hydrogen bonds in these groups allows for affinity interactions of the adsorbent with the adsorbate and is supported by polar molecules, thus improving the adsorption performance.

Methyl phenol: Compounds with a hydroxyl group attached to an aromatic ring, where the methyl group (CH_3) is attached to a phenolic or cresol ring. Cresol can generally be obtained from synthesis, biological production, and industrial processes. Because it has aromatic rings and a hydroxyl group, the formation of a stable surface can occur during the adsorption process, thereby enhancing the binding of certain adsorbates.

1.4. Charcoal

Charcoal is a highly porous form of carbon with an impressive surface area, known for its outstanding adsorption capabilities. Its porous structure offers numerous adsorption sites, thus enabling charcoal to effectively remove a wide variety of impurities and contaminants from liquids and gases. Charcoal in particular, is a type of charcoal that has undergone chemical treatment to enhance its adsorption capabilities. Activation is achievable through a range of techniques that include chemical [33] or physical methods [34]: the former entails treating it with $pH< 7$ chemicals, while the latter involves subjecting the charcoal to high temperatures. The result of the activation process creates a pore network and increases the charcoal's surface area in order to provide more sites for the adsorption process. Physical adsorption is one of the mechanisms that will occur between the adsorbate molecules and the adsorbent surface as a result of charcoal's porous structure [35,36].

1.5. Biochar

Charcoal that results from the pyrolysis of organic materials (e.g. agricultural residue, bamboo, banana peel, wood waste, or other biomass) is the material and process for obtaining biochar. Based on its high surface area and porous structure, biochar has gained attention for its potential in various applications, including water quality improvement [37]. It is pertinent that biochar's performance as an adsorbent is dependent on various factors, including the feedstock type and the properties of the specific contaminants being targeted. Fortunately, the properties of biochar can be modified through activation or functionalization to tailor its adsorption capabilities.

2. Bibliometric analysis of AC as an adsorbent

2.1. Rationale for the bibliometric analysis

Some researchers may argue that the bibliometric analysis approach is simply an observation of the presentation of research reports [38]. However, review analysis via bibliometric measures and a search engine that relies on the Scopus database (see Fig. 4) is highly efficient at determining the importance of a research focus in terms of the number and growth of articles and citations (see Fig. 5).

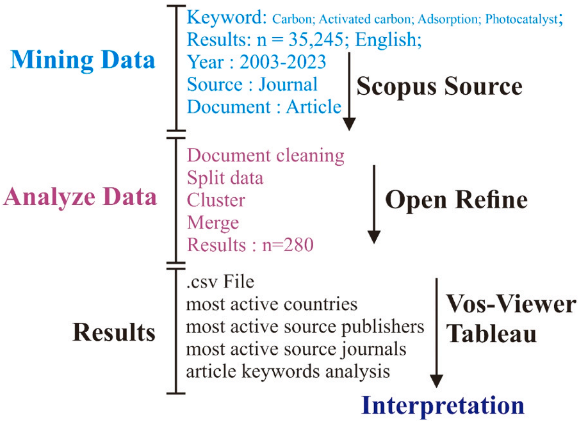

Fig. 4. The data mining process.

The data mining process commenced with keywords and resulted in 35,245 articles. This indicates that research based on AC has its own base as a waste absorber. However, when the word photocatalyst was included, there was a reduction in the number of articles to 285, which can be related to the procedure of utilizing and activating carbon. Therefore, an opportunity remains to expand the scope of implementation. The data from the article mining results were then clustered to avoid the accumulation of the same data, with OpenRefine eliminating 5 articles and thus reducing the total number of articles to 280. The findings obtained from the data mining and analysis process are the most active countries, publishers, and journals with the highest number of articles and citations, as well as the keyword relationships. Quantitative analysis of the scientific literature, including the publications, citations, and collaborations, revealed that Elsevier and journals that focus on the scope of environmental concerns dominate due to the tendency of authors to present their views and solutions for conservation.

It should be noted that most data were sourced from Elsevier B.V. and Elsevier Ltd, a leading academic publisher that demonstrates the reliability and excellence of the publication, making it a natural choice for many authors and citation decisions [39]. The sizable number of published articles ($n = 101$) indicates a noteworthy collection of works related to the topics. The articles have had a significant impact on the academic community, as evidenced by the 3150 citations that have been received.

The journal with the highest number of citations ($n = 1253$) and the most articles suggests that the publication in question is respected and well-known for its significant research publications on carbon, AC, and adsorption. The sizable number of citations indicates that the published articles make an important impact and are often referred to by other researchers. However, the second highest journal, despite having fewer articles than the highest-ranked journal, still has a considerable number of citations ($n = 455$). Based on this, it appears that the articles published in this journal received a large number of citations and made noteworthy contributions to the field. The ratio of citations to articles reflects the impact and is evidence of whether the published research is valued by the academic community.

2.2. The importance of mapping research

The need to map research focuses can relate to potential areas for further exploration. Research trends can be viewed in greater depth, and the tendency of author affiliations to focus on these areas can reveal patterns of international collaboration, indicating global interest and engagement specifically for carbon, AC, and its adsorption capacity. One of the limitations of bibliometric reviews that rely on citation and document counts is the temporal nature of the analysis, whereby the temporal evolution of publications can reveal the growth of interest in a

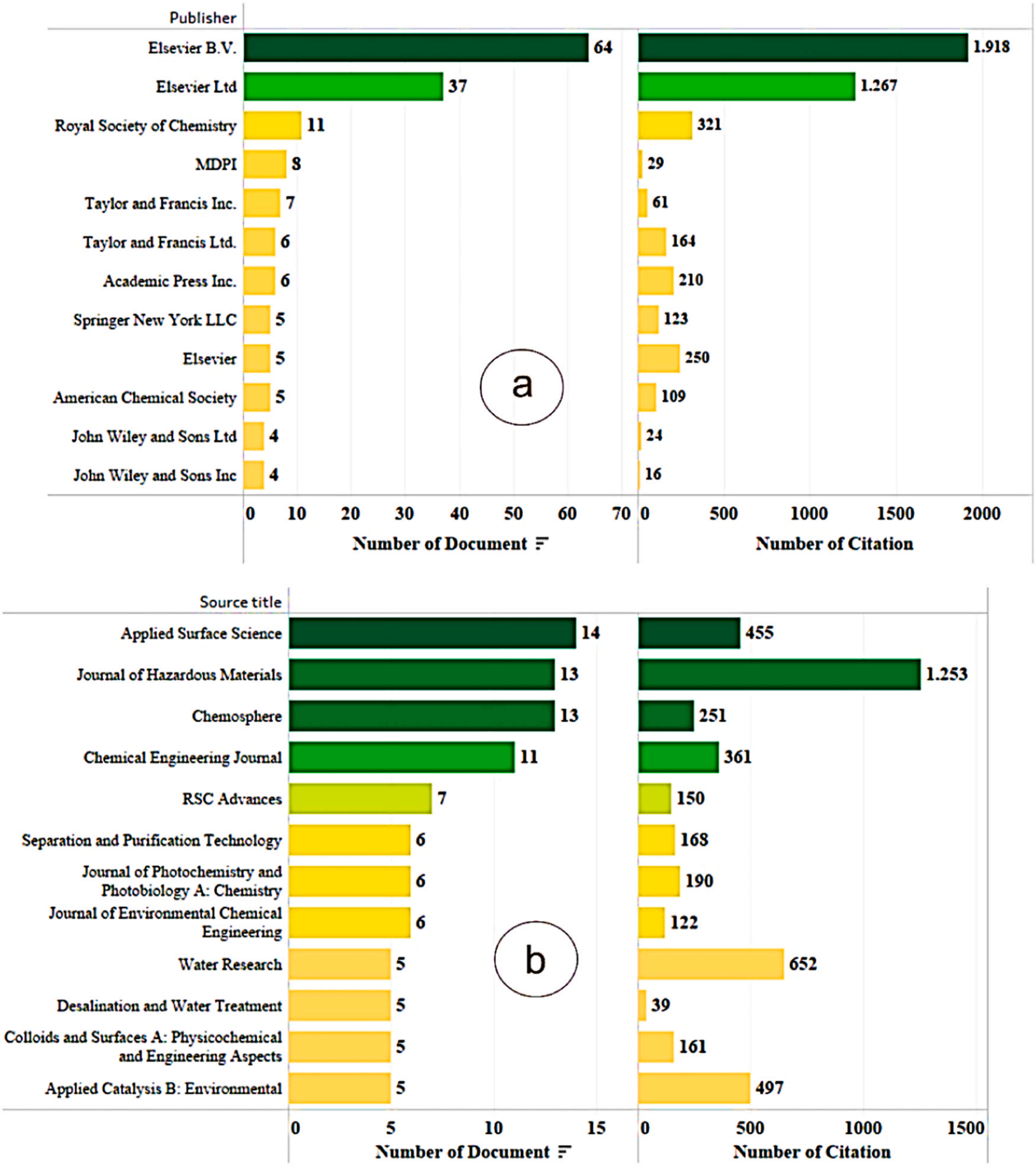

Fig. 5. (a) Publisher and (b) journal based on their count and cited status.

topic and identify periods of increased interest, but the numbers are constantly evolving. Therefore, the information mined and processed at one point in time will shift if the data mining is conducted in the future. Therefore, information on research development linked to carbon use and AC as wastewater catalysts will continue to develop according to the trend of researchers and the need for environmental preservation. Moreover, when the growth of carbon and AC-related research weakens, it will be a sign that novel materials have been discovered that are more suitable for wastewater decomposition applications. Therefore, it is useful to create a science map to recognize the transformation of research.

2.3. Collaboration, and networking keywords

One of the drivers for investigation and participation in the community is to collaborate at the international level in order to facilitate an exchange of knowledge between researchers. Collaboration between disciplines is also an important factor so that variations, innovations, and solutions to wastewater problems can be resolved, especially by using carbon and AC as adsorbents.

The country activity revealed that China and India have the largest spheres, indicating their activity in publications in this field (see Fig. 6). Meanwhile, the connecting lines between countries indicate a cooperative relationship in the form of joint publications between authors from related countries.

3. Activation method

Activation is indispensable in improving the adsorption performance of carbon adsorbents. These improvements include increased surface area [40,41], chemical properties [42,43], pore structure [44,45], adsorption capacity [46,47], and surface modification [48,49]. Table 1 shows the comparison of activation methods of several AC along with the degradation performance of various adsorbates and their adsorption

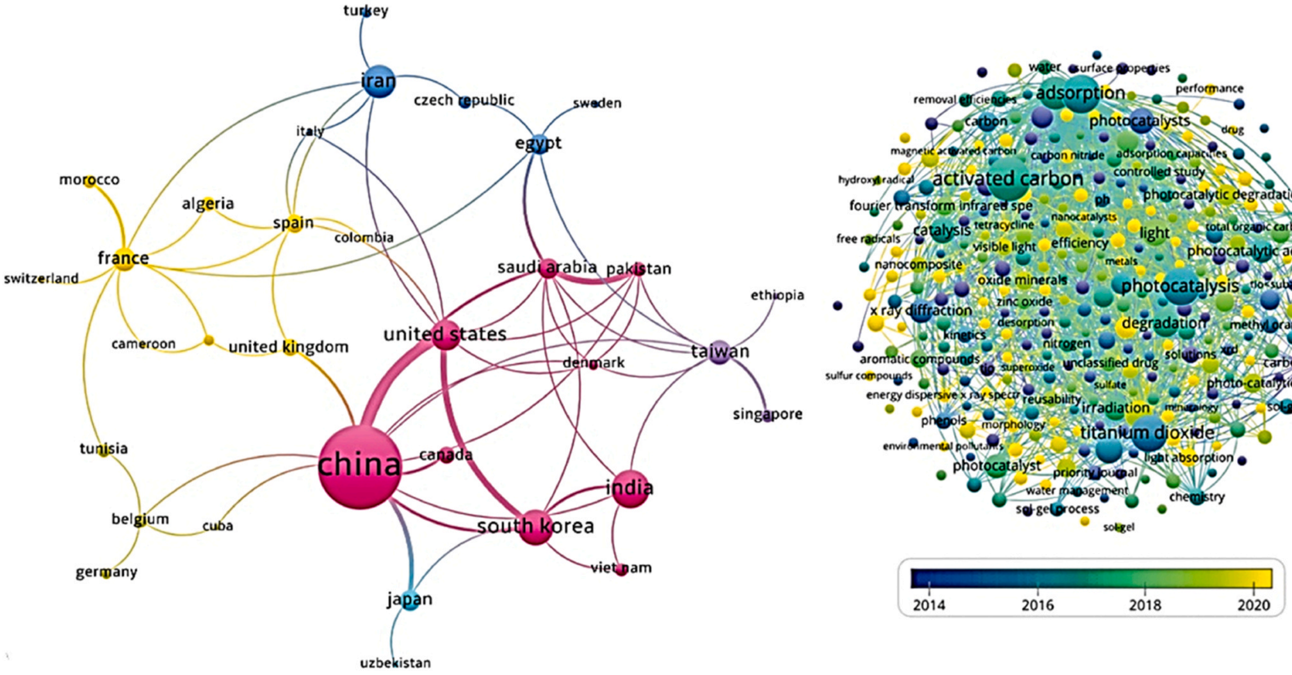

Fig. 6. The countries with a high concern for water pollution, and the keyword network.

Table 1
Performance of various activated carbons.

No	AC Source	Performance		Adsorbate	Activation Method	Ref
		Ads. capacity (mg/g)	Degradation (%)			
1	Lignin	1800	99.82	BG, α-MB, CV, MY, β-MB, and AF	Chemical	[50]
2	Raphanus seeds	10	99.4	MB	Physical	[51]
3	Biomass	330	95.87	Pazopanib	Chemical	[52]
4	Banana Peel	6	90	Pb and Cd	Pyrolysis Carbonization	[53]
5	Peanut Shells	303.03	95	MB and Pb(II)	Chemical	[54]
6	Sawdust	10	99.69	MO and MR	Chemical	[55].
7	Durian Skin	50	91.49	MB	Chemical	[56]
8	Sunflower Stem	365.81	90	Phenol and Bisphenol A (BPA)	Chemical	[57]
9	Rice Straw	300	95	MB	Synthesized Activation	[58]
10	Goat-Weed	100	93	Hospital Wastewater	Pyrolysis Chemical	[59]
11	Biomass	1096.31	99.58	Glycerol	Chemical	[60]
12	Waste Newspaper	651	89.6	MB and CR	Chemical	[61]
13	Biomass	916.3	93.2	Almotriptan and Paracetamol	Chemical	[62]
14	Ice Cream Wastewater	588.23	98.6	RhB and AR97	Physical	[63]
15	Coconut Shell	15,827	98	Oils and Organic Solvents	Chemical	[64]
16	Musa paradisiaca Peel	20	98.23	Hexachlorocyclohexanes	Chemical	[65]
17	Biomass	6	97.6	Tetracycline	Chemical	[66]
18	Commercial	5.056	40	Ammonia	Chemical	[67]
19	Pinewood	25	95	Diclofenac and Ciprofloxacin	Chemical	[68]
20	Sawdust	512	73	Textile Dyeing Industry (direct blue, green, and orange)	Chemical	[69]

capacity.

3.1. Physical activation

The principle of porous structure formation for natural materials has common stages such as carbonization, temperature ramp-up, and activation duration. The carbonization of raw materials, which involves the decomposition of complex organic molecules into carbon-rich structures, is generally carried out at temperatures in the 600–900 ℃ range. Similar to the carbonization process, temperature ramp-up is a higher heating to > 950 ℃, where the application of temperature must be controlled to avoid thermal shock. Structural transformation, and the formation of micro- and mesopores, are processes that the material will undergo due to the removal of complex organic molecules so that components such as water, gas, and tar separate and ultimately leave the element carbon [70]. In certain cases, a porous structure formation may still be maximized by selecting the appropriate activation duration. Therefore, the length of the activation duration is actually highly dependent on the source material being activated. However, it should be noted that a long activation duration will generate low adsorption capacity and require high energy consumption [71].

3.2. Chemical activation

Chemical activation can be deemed as a complementary step to physical activation. After obtaining a porous surface structure, the porosity level is the next concern. Increasing the porosity properties of the material can be obtained through acid solutions to neutralize any remaining alkaline substances. Phosphoric acid [72], potassium carbonate [73], sodium hydroxide, and zinc chloride [74] are activators that have been applied to activate AC.

3.3. *Factors influencing the degradation performance*

Factors such as the temperature, adsorbent dosage, pH, contact time, initial pollutant concentration [75,76], and wavelength matching are important variables that are often reported as determining the quality of a study related to photocatalysts [77], and are of course associated with the produced AC's quality and the pollutant type targeted.

Wavelength matching warrants being one of the determining factors for the success of adsorption processes that utilize the light spectrum. Photocatalyst reactions such as AC have been widely reported as active in the UV region, and clearly activeness in long spectral ranges will provide greater opportunities for the generation of electron and hole pairs [78]. The suitability of the pH value also cannot be ignored in the photocatalysis process, since each adsorbent has a suitable pH of ~7.5, ~6, and ~4 that makes the degradation process optimal [77,79]. The contact time refers to the length of the adsorbate–adsorbent interaction period [80]. In terms of the interaction behavior, greater duration allows more impurity molecules to interact with the photocatalyst, leading to increased degradation. However, the reversal process in a condition can be a matter of concern as results of increasing and decreasing percentages of degradation per length of time have been widely reported [81]. A suitable interaction duration can achieve a balance between the adsorption of impurities on the photocatalyst surface, and their subsequent degradation.

Photocatalysts can change over time, which affects their efficiency in degrading impurities. The pollutants' initial concentration and the adsorbent's mass are two factors that can maintain the stability of their interaction, so that effective degradation can be obtained. Increasing the amount of the initial pollutant concentration as an adsorbate source will increase the adsorption capacity until the process reaches saturation; otherwise, a small amount of dye can cause interaction restrictions, resulting in repeated reactions [82]. Meanwhile, adsorbate removal is raised through an increased adsorbent dosage as it enhances the probability of surface adsorption sites [83]. Therefore, the dosing factor is also a concern for researchers seeking favorable research outcomes in this field.

The stability of carbon and AC is an important aspect in various applications. Studies have shown that biomass-derived AC exhibits excellent stability and regeneration ability, rendering it suitable as an adsorbent [84]. In addition, the use of natural waste materials in the manufacture of carbon adsorbents and AC not only improves their stability but also contributes to environmental sustainability [85]. Overall, carbon and AC adsorbent materials show stability in the effectiveness and longevity of adsorbents, indicating their versatility in various industrial applications.

3.4. *Adsorption modeling and optimization*

3.4.1. *Response surface methodology*

The response surface methodology (RSM) is a mathematical and statistical technique for designing experiments to optimize processes in terms of interacting variables and evaluating the responses to optimize the outcome information from a system. In the context of adsorption modeling and optimization, RSM is applied using various factors such as the adsorbate concentration, adsorbent material type, and interaction duration so that the role of these factors can be systematically explored [86]. In its implementation, there are two variables used: independent and dependent. The second-order polynomial is a mathematical model that fits the experimental design data and follows the following equation:

$$Y = \beta_0 + \sum_{i=1}^{k} \beta_i x_i + \sum_{i=1}^{k} \beta_{ii} x_i^2 + \sum_{i=1}^{k-1} \sum_{j=2}^{k} \beta_{ij} x_j x_i + \varepsilon \tag{1}$$

Design–Expert is software that can be employed to perform the RSM model. The input variables can be adsorbent, contact time, initial dye concentration, and pH, while the adsorption efficiency is the target output [87].

The RSM approach can be updated with an artificial neural network (ANN) approach to model cationic dye removal by adsorption. As reported by Ozcelik *et al.*, the application of RSM was utilized to enable the evaluation of the process via four controllable operating parameters [88]. With the inputs of adsorbent dosage (0.1–0.5 g), contact time (10–90 min), initial dye concentration (50–150 mg/L), and pH (3–9), a regression model ($R = 0.9714$) was obtained indicating that the regression was satisfactory and thus represented a promising model.

3.4.2. *Artificial neural network*

ANNs are utilized for classification, optimization pattern recognition, and regression tasks by learning from data and utilizing computational models inspired by the functioning of the human brain. Through the use of components from statistical learning algorithms that are based on neuronal systems, ANNs can be developed into multi-layer perceptron ratification ANNs (MLP-ANNs), the role of which in the context of adsorption modeling and optimization is capturing the relationships of complexity within the input variables that affect adsorption performance and the response variables, such as efficiency (see Fig. 7). ANNs are often the modeling of choice due to their high adaptability to system changes, as they can continuously learn while new data become available, making them suitable for applications where adsorption processes may evolve over time [89]. For improvement, the normalization of the input data for ANN models typically involves converting the dataset into a standard scale with a range of [0 1], thus requiring several three-part components that are organized into training, testing, and validation datasets [90].

3.4.3. *The role of density functional theory in the adsorption process*

Prior to the development of density functional theory (DFT) by Kohn and Sham, scientists relied on the Schrödinger equation to study electrons. DFT has gained popularity in material design thanks to its ability to handle interacting electrons and account for certain corrections in the material [91]. Fig. 8 illustrates the development of the time-dependent DFT (TDDFT) approach to solving complex problems involving multiple particles, which eventually led to the widespread use of DFT [92,93]. This discussion explores how the Schrödinger equation has been employed in materials design, while also highlighting the importance of certain quantum physics principles in running simulations that aid material development, especially in adsorbents and fields such as drug delivery [94,95], photocatalysts [96,97], energy storage [98,99], and spacecraft coatings [100].

The important role of DFT in understanding the performance of adsorbents such as carbon and AC can be divided into two parts of the mechanism: simulating adsorption, and designing and optimizing adsorbents.

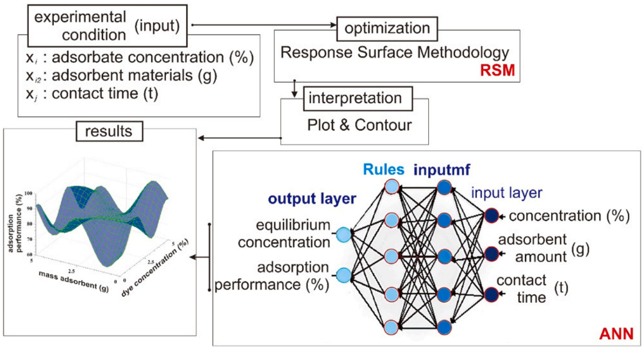

Fig. 7. RSM and ANN principles to obtain adsorption performance.

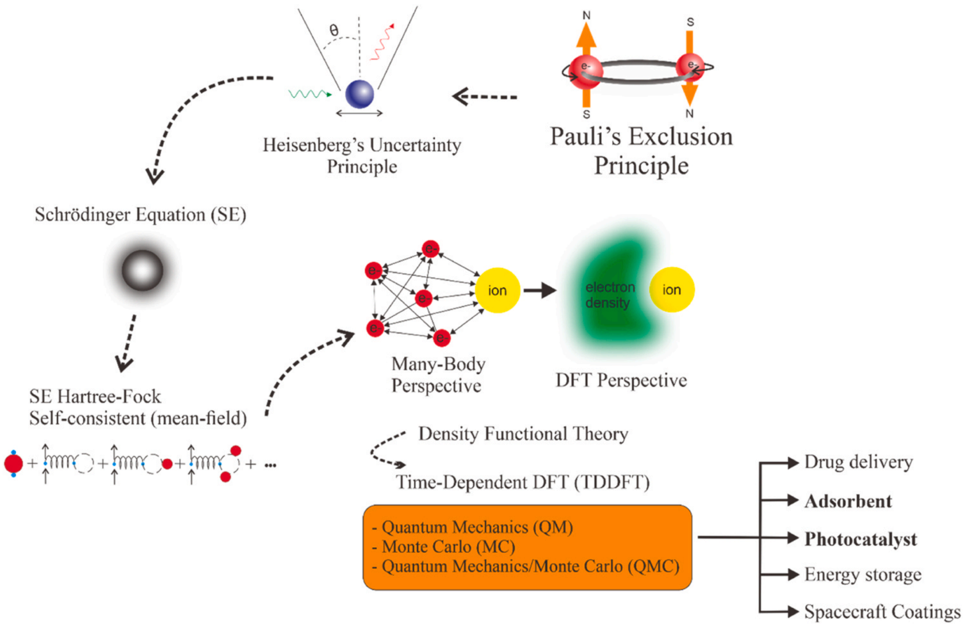

Fig. 8. The DFT journey and its rules are to be implemented in several fields.

3.4.3.1. Simulating adsorption. Wei *et al.* [101] reported a type of AC (ENAC) by treating macroalgae (Enteromorpha clathrate) with sodium hydroxide (NaOH). The new material has a very large surface area of 1238,491 m^2 per gram, as well as a significant total pore volume of 0.6823 cm^3 per gram, with an average pore size of 2.2038 nm. The researchers conducted adsorption modeling, thermodynamics, and DFT simulations of tetracycline on mesopores, which showed electrostatic interactions, π-π interactions, and hydrogen bonding between the adsorbent and pollutants. Their results confirmed that the fabricated ENAC has promising application prospects in removing antibiotics from aqueous solutions, and their simulations were conditioned with all energy information (electronic energy and Gibbs free energy) corrected to zero-point energy [102].

3.4.3.2. Designing and optimizing. The combination of DFT and molecular dynamic simulations has been reported as a powerful method and demonstrated in the study of SO_2 and CO_2 adsorption on graphite (111) surface in an aqueous medium [103]. The description included the overall electronic structure of the material with the energies of the highest occupied and lowest unoccupied molecular orbitals, the energy gap between them, hardness, softness, electron transfer, and electronegativity. The calculation strategy was performed with the Gaussian 09 W program package employed for DFT calculations, while the molecular dynamic chemical descriptor was calculated via the adsorption tracer module (Accelrys, San Diego, CA, USA) implemented in Material Studio 8.0, which is distributed by the BIOVIA community and used to build substrate systems [104].

3.5. Isotherm models

The mathematical representation between adsorbed adsorbate and the adsorbate's equilibrium concentration in the fluid phase is isotherm modeling, which helps characterize the adsorption behavior because it understands how adsorbate molecules interact with the adsorbent surface. Furthermore, it measures the maximum adsorption capacity and adsorbent as it provides the mass adsorbed or the mass/volume of adsorbent adsorbed at equilibrium conditions.

3.5.1. Two parameter isotherm model

3.5.1.1. Langmuir model. Introduced in 1918 by Irving Langmuir, the Langmuir model assumes that adsorption occurs on a homogeneous surface with a finite distribution of identical, non-interactive adsorption sites. Since this model describes a chemisorption event, the rate of adsorption equals the desorption rate: $q = \frac{Q_{\max}.C}{1+K.C}$. The adsorption rate $(k_1[A][S])$ and desorption rate $(k_2[A - S])$ change according to the function of q_e, so that the equations become $k_1 C_e(1-q)$ and $k_2(q_e)$, respectively, along with the development of nonlinear and linear Langmuir models that can be obtained by entering the $q_{\max}$ variables [105]:

$$q_e = \frac{q_{\max} k_L C_e}{1 + k_L C_e} \text{for nonlinear models} \tag{2}$$

$$\frac{C_e}{q_e} = \frac{C_e}{q_{\max}} + \frac{1}{q_{\max} k_L} \text{for linear models} \tag{3}$$

where $k_L = \frac{q_e}{(1-q_e)C_e}$, and thus it is possible to express the adsorption capacity on the surface through the Langmuir splitting factor, which is defined as [106]:

$$R_L = \frac{1}{1 + K_L C_0} \tag{4}$$

The characteristics of the adsorption process can be briefly obtained through the following conditions:

$$(R_L > 1)\text{indicatesunfavorable adsorption, if}(R_L = 1)\text{indicateslinear adsorption} \tag{5}$$

$$(0 < R_L < 1)\text{indicatesfavorable adsorption, if}R_L = 0\text{indicatesirreversible adsorption} \tag{6}$$

Freundlich model: In 1906, Herbert Freundlich proposed this model for consideration. When compared to the Langmuir model, the Freundlich model is not based on monolayer adsorption occurring on a completely uniform surface. Rather, this model allows diverse surfaces to engage in multilayer adsorption. It should be noted that its behavior may deviate from Henry's law when observed under low pressure. The empirical equations of the Freundlich model also include nonlinear models such as the Langmuir model, which can be presented as follows:

$$q_e = K_F C_e^{1/n} \text{for nonlinear models} \tag{7}$$

$$\ln q_e = \ln k_F + \frac{\ln C_e}{n} \text{for linear models} \tag{8}$$

The provisions in Eqs. 7 and 8 are as follows:

$$\left(0 < \frac{1}{n} < 1\right)\text{indicates desirable, if}\left(1 < \frac{1}{n}\right)\text{indicates undesirable adsorption} \tag{9}$$

and

$$\left(\frac{1}{n} = 1\right)\text{indicates irreversible adsorption} \tag{10}$$

The factors of temperature and adsorption intensity affect the change in the variables K_F and $1^{1/n}$. The high temperature corresponds to a high K_F, revealing the thermodynamic relationship between them. Meanwhile, the high intensity indicates the nonlinear weakening of $1^{1/n}$, which points to the adsorption concentration as the cause of the phenomenon [107]. In the comparison between optimization techniques to determine the performance of photocatalysts, there are several methods as shown in Table 2.

The equations associated with adsorption isotherms essentially predict the adsorbed amount as a function of concentration at constant temperature. Temkin, Halsey, Jovanovich, Harkins–Jura, and Liu are isotherm models that are of practical use for researchers. Modelling that describes the relationship between adsorbate molecules on an inhomogeneous surface is the basis of the *Temkin model*. The formulation that q_e is directly proportional to RT is based on the assumption that there is a linear decrease in the adsorption heat with increased coverage as a result of the adsorbate molecules' interaction, or vice versa. It should be noted, however, that this model ignores the adsorbate concentration, thus limiting its application to intermediate ion concentrations [117]. The *Halsey model* assumes adsorption energy on an heterogenous surface, where a heterogeneous surface resulting from a collection of monolayer adsorption capacities has a linear relationship with the amount adsorbed. In other words, this model describes multilayer adsorption if the temperature distribution is not uniform. Considering the equation shown in Table 1, the *Jovanovich model* represents modelling that conforms to the Langmuir assumption. This model is used for monolayer adsorption, and is based on the equation $(e^{K_J C_e})$ whereby the model will reach equilibrium at an elevated concentration. In terms of mechanical interaction, the attraction and repulsion forces between the adsorbed molecules can be observed in K_J as a representation of the interaction intensity. The *Harkins–Jura model* is essentially a statistical and non-mechanistic model that does not produce direct linear or nonlinear equations, as per some empirical adsorption models, and tends to be more of a conceptual model that describes the distribution of adsorption energy on a heterogeneous surface [118]. The *Elovich model* described by $\left(\frac{q_e}{e^{q_m}}\right)$ appears to assume an exponential decrease in the adsorption rate with surface coverage. The adsorption phenomenon is considered to have slowed down because it initially has a high reaction speed and along with the contact time there is a deceleration that may be caused by the empty sites that have been filled so that the adsorbed molecules' interaction starts to become limited [119]. The combination of a limited number of monolayer binding and adsorption sites with heterogeneous surface energy and non-ideal interactions between adsorbed molecules constitutes the *Liu model,* which on the basis of this statement is often said to be a Langmuir–Freundlich combination [120].

Table 2
Determining the q_e and q_t through isotherm and kinetic models.

Isotherm model	nonlinear	linear	Ref.
Temkin	$q_e = \frac{RT}{b}\ln(K_T C_e)$	$q_e = \frac{RT}{b}\ln(K_T) + \frac{RT}{b}\ln(C_e)$	[108]
Halsey	$\ln q_e = \left(\frac{1}{n_H}\right)\ln K_H - \left(\frac{1}{n_H}\right)\ln C_e$	$q_e = e^{\frac{\ln K_H - \ln C_e}{(n_H)}}$	[109]
Jovanovich	$q_e = q_{\max}(1 - e^{K_J C_e})$	$\ln(q_e) = \ln q_{\max} - K_J C_e$	[110]
Harkins–Jura	$q_e = \left(\frac{A_{HJ}}{B_{HJ} - \log C_e}\right)^{1/2}$	$\frac{1}{q_e^2} = \frac{B_{HJ}}{A_{HJ}} - \left(\frac{1}{A_{HJ}}\right)\log C_e$	[111]
Elovich	$q_e = q_m K_e C_e e^{\frac{q_e}{q_m}}$	$\ln\left(\frac{q_e}{C_e}\right) = \ln K_e q_m - \frac{q_e}{q_m}$	[112]
Liu	$q_e = \frac{q_m (k_{liu} C_e)^{n_g}}{1 + (k_{liu} C_e)^{n_g}}$	$\frac{t}{q_t} = \frac{1}{k_1 q_e^2} + \frac{t}{q_e}$	[113]
Kinetic model	**nonlinear**	**linear**	
Pseudo-first order	$q_t = q_{em}(1 - e^{-K_1 t})$	$\ln(q_{em} - q_1) = \ln(q_{em}) - k_1 t$	[114]
Pseudo-second-order	$q_t = \frac{k_1 t q_{em}^2}{1 + k_1 t q_{em}}$	$\frac{t}{q_1} = \frac{1}{k_1 q_{em}^2} + \frac{t}{q_{em}}$	[115]
Intra-particle diffusion	$q_t = K_{\text{int}}\sqrt{t} + C_{\text{int}}$	Not reported	[116]

The kinetic adsorption model focuses its attention on how the speed that the adsorbate in bulk or solid form that has surface interactions binds to the adsorbate. Reaction kinetics are presented as reaction rates that are dependent on several factors including the initial adsorbate, temperature, and competing solutes being present, with 10^{-9} s^{-1} representing the highest rate currently known. The assumption of an adsorption rate proportional to the available vacant sites generally occurs through a chemisorption process, often referred to as the *Pseudo-first-order model.* Chemisorption leads to the formation of a strong chemical bond between the adsorbate and the adsorbent, where the adsorbent surface is considered homogeneous, meaning that all the active sites have identical binding energy. Meanwhile, the model that considers the occupied and unoccupied locations through the process of physisorption is called the *Pseudo-second-order model.* Physisorption perceives the adsorption rate as proportional to the product of occupied and unfilled active sites dominated by van der Waals forces or hydrogen bonding, leading to a weak reaction. In this model, the adsorbent surface is considered heterogeneous, and thus different active sites may have different binding energies. The *intra-particle diffusion model* is a description of the adsorption rate and the factors affecting it such as the equilibrium between the adsorbate concentration and the amount adsorbed. This model has a good capacity to understand adsorption kinetics, specifically in the case of adsorbate molecules' diffusion within the adsorbent pores.

3.6. *Implementation of carbon and AC for various research fields*

3.6.1. *Civil engineering*

Carbon-based materials like carbon black (CB), carbon fiber (CF), and carbon nanotubes (CNTs) are promising materials for civil engineering because of their high strength and durability, sustainability, energy efficiency, and versatility [121–123]. Khan *et al.* utilized CF reinforced polymer (CFRP) wrapping to confine reinforced concrete (RC) columns, leading to a notable augmentation in their load-carrying capacity [124]. Through comprehensive investigations, it was discovered that employing CFRP wraps for column confinement was not only effective in enhancing the load-carrying capacity (increased by 64.75 % and 19.55 % compared to the control plane and RC columns, respectively) but also prevented steel reinforcement yielding and concrete crushing in the steel core region. The utilization of CFRP is becoming more prevalent in the reinforcement and restoration of structural elements including columns, beams, slabs, and shear walls. Incorporating CFRP into these components offers engineers the opportunity to enhance their durability, load-bearing capacity, and seismic resistance while simultaneously lowering their mass and dimensions [125].

Jung *et al.* [126] incorporated CNTs into ultra-high-performance concrete (UHPC) and examined their dispersion, electromagnetic shielding effectiveness, and mechanical characteristics. The conducted experiments demonstrated that the inclusion of CNTs enhances the UHPC's mechanical properties by facilitating bridging, pore filling, and promoting a denser C–S–H structure. Moreover, the addition of CNTs significantly enhances the electrical conductivity and consequently improves the Schrödinger equation up to the percolation threshold.

CB nanoparticles (CBNPs) were utilized as reinforcement in asphalt mixtures by Rafi *et al.* [127]. Experimental results have shown that the optimal CBNP dosage in asphalt is 10 % by bitumen weight. CBNP addition to asphalt binder has resulted in stiffer asphalt mixtures that have superior rutting resistance at elevated temperatures. Additionally, a significant bitumen–aggregate bond strength improvement was observed with the incorporation of CBNPs.

Lekkam *et al.* [128] reported saturated AC's (SAC) influence on cementitious materials' mechanical and rheological characteristics, with their study proposing a novel approach focused on the potential reuse of SAC as a cementitious material additive. They prepared eight mixtures comprising four pastes and four mortars, each with varying AC waste percentages (0.5 %, 1 %, 2 %, and 4 %), where a comparison was made with a reference mixture. Their findings indicated SAC's effective utilization as an organic additive in cementitious materials with no compromise to the mechanical strength and fluidity, provided that the substitution percentage remains below 2 %.

Annamalai *et al.* [129] reported phenol-contaminated soil's remediation using persulfate activated by ball-milled colloidal AC (CACBM), finding the degradation efficiency of phenol in field-contaminated and spiked soils through a new, low-cost CACBM catalyst. Remarkable phenol degradation performance was exhibited by the CACBM/persulfate system in both field-contaminated and spiked soils.

3.6.2. Energy storage

Carbon-based materials, renowned for their cost-effectiveness, electrical conductivity, environmental friendliness, high surface area, mechanical and chemical stability, and tunability, are widely utilized in energy storage. From graphene to AC and carbon composites, these materials optimize ion adsorption and electron transport in batteries and supercapacitors, ensuring efficient energy storage and delivery while offering customizable solutions to meet diverse application needs [130–132].

Sahoo *et al.* [133] detailed recent advancements in graphene-based nanomaterials incorporating carbides, conducting polymers, metal oxides, nitrides, phosphides, and sulfides. These nanocomposite materials leverage the synergistic effects of graphene's large surface area, enhanced conductivity, and the high pseudo-capacitance properties of metal oxides, nitrides, sulfides, carbides, phosphides, and conducting polymers. Consequently, graphene-based nanomaterials emerge as exceptional electrode materials for supercapacitors, and regarding cyclic retention, energy density, power density, and specific capacitance they surpass their individual components.

Jia *et al.* [134] successfully encapsulated hollow Co_9S_8 nanoparticles (CS) within N, S co-doped carbon nanotubes (NSCNT), forming an advanced electrode for supercapacitors and sodium-ion batteries (SIBs). The resulting CS-NSCNT^{-3} electrode has exceptional capacity, rate capability, and reversibility. In supercapacitors, the CS-NSCNT electrode achieves a high specific capacitance of 1150 F/g at 1 A g^{-1}, coupled with remarkable cycling stability and rate performance. Similarly, in SIBs, the CS-NSCNT cathode displays an initial reversible capacity of 475 mAh g^{-1} at 0.1 A g^{-1}, and retains 53 % capacity at 10 A g^{-1}, offering superior rate performance. The research addresses the future application requirements for high capacitance/capacity, high-power/energy density, and long-term stability.

Anand *et al.* [135] developed walnut shell-derived highly porous heteroatom (nitrogen and sulfur)-doped AC (NS-WAC) through KOH activation and subsequent post-processing treatment using thioacetamide. NS-WAC boasts a diverse particle size distribution (featuring micro-, meso-, and macro-pores) and a high specific surface, which impart significant benefits for supercapacitors. NS-WAC is characterized by electrochemical performance of great promise, with a high gravimetric specific capacitance of 271.4 Fg^{-1} at 0.5 Ag^{-1} achieved in a 3 M KOH aqueous electrolyte.

Jeon *et al.* [136] successfully improved sodium ions' interdiffusion behavior and electrochemical performance in an onion-derived freeze-dried and KOH-AC for SIB anodes. Utilizing a facile activation and annealing process in combination with freeze drying and KOH treatment, nitrogen-doped onion-derived carbon materials (dried onion (DO) and freeze-dried onion (FDO)) with high specific surface areas were prepared. The resulting carbon materials offered superior electrochemical performance as SIB anodes, with the delivery of high discharge reversible capacities of 140.5 mAh/g (DO) and 151.4 mAh/g (FDO) at a 0.05 A/g current density after 30 cycles. Moreover, the capacities reached 45 mAh/g (DO) and 66 mAh/g (FDO) at 30 A/g. Notably, FDO//Na3V2(PO4)3 @C full cells attained a 43.9 mAh/g reversible capacity with a specific energy of 91.5 Wh kg^{-1} at 5 C following 1000 cycles, suggesting promising application for SIB energy storage systems.

Chaudhary *et al.* [137] conducted a review of porous AC materials derived from various forms of biomass, with AC's biomass sources and electrochemical properties revealed. In the energy storage application domain, utilizing bioresources such as bamboo waste, banana peel, datura, green tea waste, lotus stems, pineapple leaves, waste tires, and wood as AC demonstrates considerable supercapacitor energy storage capabilities, with specific capacitances reported to reach up to 1400 F/g. Additionally, the functions of batteries and supercapacitors are highlighted, alongside the different energy storage roles played by each component.

3.6.3. Biomedical application

Adsorption and enrichment play crucial roles in various aspects of biomedicine, such as blood purification, breath analysis, and enriching specific biomolecules [138]. These processes rely on the use of adsorptive materials that capture target molecules, ultimately supporting disease diagnosis and treatment [139,140]. Research heavily focuses on designing and creating adsorbent materials with specific microstructures and physicochemical properties tailored for desired applications [141]. Carbon materials stand out as attractive candidates due to their excellent mechanical strength, high surface area, biocompatibility, and ease of modification. Notably, the diverse forms of carbon (0D to 3D) further broaden their potential in biomedicine [142]. AC, biomass/polymer-derived carbon, carbon-based quantum dots, CNTs, and graphene and its derivatives represent commonly employed carbon materials [143]. Advanced fabrication techniques enable the precise crafting of these materials into various structures to address specific biomedical adsorption and enrichment requirements [144]. Carbonaceous materials have proved to be promising choices for adsorption or enrichment media in a range of biomedical applications such as breath analysis, blood purification, glycopeptide or phosphopeptide enrichment, due to their exceptional mechanical performance, high specific surface area, environmental friendliness, and ability to be easily surface-modified [145]. Purifying patients' blood is essential to removing excess toxins, pathogens, and waste products, which are vital for disease therapy. The use of adsorbents in hemoperfusion is an effective method for purifying blood. Therefore, there is a high demand for superior sorbent materials possessing cost-effectiveness, excellent hemocompatibility, a large specific area, and notable selectivity. Hemoperfusion is indicated for conditions such as acute drug or toxic poisoning, acute liver failure, chronic kidney disease, and severe hepatitis. Carbon-based materials offer promising sorbents for hemoperfusion due to their excellent performance in various aspects. Typically, these materials can be combined with polymers to produce adsorbents with satisfactory mechanical strength and exceptional toxin-removal efficacy from blood [146–148]. Graphene oxide (GO) composite bead adsorbents coated with cellulose acetate (CA) were developed by Tyagi *et al.*, aiming to eliminate both uremic toxins and bilirubin from blood [149]. More specifically, the in vivo investigations validated their exceptional capacity to eliminate excess creatinine and uric acid. Furthermore, molecular dynamic simulations demonstrated that the CA-functionalization enhanced surface coverage and uric acid and creatinine binding. In order to eliminate bilirubin, Du *et al.* created mesoporous–microporous composite beads using cellulose and CNTs via a micelle template [150]. Remarkably, the target molecules were able to diffuse through the macropores, leading to a high adsorption capacity and quick adsorption kinetics. Heparin–mimetic biomacromolecules were incorporated into reduced graphene oxide rGO nanocomposite spheres by Song *et al.* [151], with the resulting rGO-based sorbent able to significantly lower the risks of bleeding associated with the directed use of anticoagulants, while avoiding blood clots from forming.

AC has emerged significantly as a versatile tool in the biomedical field in recent years, offering a number of benefits, not least its purifying effect and detoxifying properties. It purifies the body as a complement to a varied diet, and acts as a detoxifier in cases of drug overdose, mild heavy metal poisoning, or poisoning. For intestinal disorders, AC regulates transit and soothes diarrhea, gastroenteritis, and constipation linked to intestinal fermentation. Moreover, it is effective in relieving digestive disorders such as heartburn, gastric reflux, aerophobia, flatulence, bloating, belching, irritable bowel syndrome, and cramps due to the excessive consumption of fats and sugars. AC also helps lower blood cholesterol and triglyceride levels, and eliminates bad breath (halitosis), while remaining a common recommendation for resuscitation and the emergency treatment of acute poisoning in many countries due to its detoxifying properties [152]. In the case of ingesting a potentially toxic dose of a substance, several poison control centers recognize treatment with activated charcoal through the administering of a single dose to reduce the absorption of the toxic substance. AC is most effective when administered rapidly, preferably within one hour of ingestion. It is also being studied in the field of nephrology for its potential in the treatment of renal failure [153], with several scientific studies confirming its value as a complementary treatment for certain aspects of the management of chronic renal failure. For example, hyperphosphatemia, commonplace in end-stage renal disease, is linked to higher morbidity and mortality, leading to secondary hyperparathyroidism. A study conducted by Wang *et al.* evaluated the effects of activated vegetable carbon on reducing serum phosphorus levels in hemodialysis patients, where the results demonstrated that activated vegetable carbon effectively controls hyperphosphatemia and hyperparathyroidism in chronic renal failure patients treated with hemodialysis [154]. A study by Tominaga *et al.* examined AC's efficacy in treating bacterial vaginosis and its effects on vaginal flora. Patients with bacterial vaginosis were allocated into two groups: one received intravaginal tampons containing a 10 % activated charcoal solution, while the other group was treated with a chloramphenicol vaginal ovule (100 mg). The results showed that in terms of the chloramphenicol-treated patients, lactobacilli disappeared in 84.3 % of women, while only 3.1 % of the activated charcoal-treated group showed this loss, with the difference of statistical significance. In addition, both treatments led to a reduction in vaginal secretions and an improvement in odor [155]. In regard to the use of AC in cardiovascular disease, several studies have confirmed its beneficial effects on lipid parameters, in particular its cholesterol-lowering effect. Activated charcoal is currently widely employed in hospitals around the world to treat intoxication and poisoning, whether due to drugs, medication overdose, food, or the ingestion of household products. It is also used in other medical fields such as nephrology, gastroenterology, pediatrics, and cardiology, and is a common pharmacological tool in veterinary medicine [145].

3.6.4. Electronic and sensor

A biosensor is a device that utilizes a biological sensing component connected to a transducer, which converts physical or chemical changes into measurable signals. These signals, typically electronic, correlate with the concentration of specific chemicals. The effectiveness of biosensors is heavily reliant on the materials used in their fabrication [156]. Carbon-based materials such as carbon dots (CDs), CNTs, graphene oxide, and graphite paste are widely employed in biosensor construction due to their capacity for surface regeneration, cost-effectiveness, ease of fabrication, and low background current. The high conductivity and porosity of certain carbon materials render them well-suited for the adsorption of large molecules and electrochemical signal transduction [157].

Carbon's ability to exist in various forms such as graphite, diamond, Q-carbon, graphene, and CNTs makes it versatile for bio detection applications [158]. Graphene has a specific surface area of 2630 m^2 g^{-1} and a thermal conductivity of 5000 W m^{-1} K^{-1}. CNTs and graphene exhibit high electrical conductivity, with values reaching 106–107 S/m for pure CNTs and 108 S/m for pure graphene. Additionally, CNTs have a significant surface area of approximately 1000 m^2/g. Carbon-based biosensors can detect a wide range of environmental analytes including toxic vapors, neurotoxic agents, and peroxides, as well as drugs, proteins, and biomarkers. Researchers are thus exploring new methods to produce these carbon polymorphs for enhanced bio detection capabilities [159,160].

Pirsaheb *et al.* reported the recent applications of CD-based biosensors in detecting cancer markers and imaging cancer cells. Despite promising performance in biomedical research, transitioning CDs from scientific inquiry to clinical use faces challenges, particularly the need for human clinical trials. Furthermore, despite considerable research on CDs for bioanalytical detection, there is a paucity of reports on constructing highly sensitive CD detection systems on solid platforms [161]. Fig. 9 presents the implementation of carbon and AC in various fields based on the selection of their structure and properties.

Arshad *et al.* conducted research regarding the use of graphene and its derivatives to develop biosensors capable of detecting cancer biomarkers with high specificity and reproducibility, discussing various methods to transform graphene and its derivatives into diagnostic platforms applicable for both imaging and therapy. However, while graphene-based biosensors show immense potential for early and optimal cancer diagnosis, and can simultaneously detect different cancer biomarkers in samples, their toxicity raises health concerns. Therefore, further research is needed to optimize these graphene-based biosensors and render them suitable for real-world clinical applications [162]. The near-infrared emission, photostability, and sensitivity of CNTs make them ideal candidates for the development of optical sensors and bio detection applications. Williams *et al.* developed a sensitive and specific fluorescent biosensor using the optical properties of CNTs for the detection of the metastatic prostate cancer biomarker, urokinase plasminogen activator (uPA) [163]. Photoluminescent single-walled CNTs were modified to specifically respond to uPA by antibody conjugation, through which the modulation of the optical bandwidth is controlled by the analyte interaction. The DNA/aptamer–CNT platform yielded improved results for the detection of the CA125 cancer biomarker with a fluorescent biosensor using three-dimensional CNTs immobilized by an anti-CA125 antibody [164]. Therefore, further research is needed to optimize these carbon-based biosensors and make them suitable for real-world clinical application.

The conductivity of AC that changes in the presence of certain gases makes it a potential candidate for building sensor electrodes, whereby the principle of the sensor is detecting changes in conductivity after exposure to the target gas to be measured, in order to indicate its presence. AC has demonstrated its ability as a base material for biosensor design due to its high surface area, low cost, and sustainability, with Fatoni *et al.* developing a glucose biosensor, as well as for the non-invasive determination of uric acid in saliva [165]. Even the use

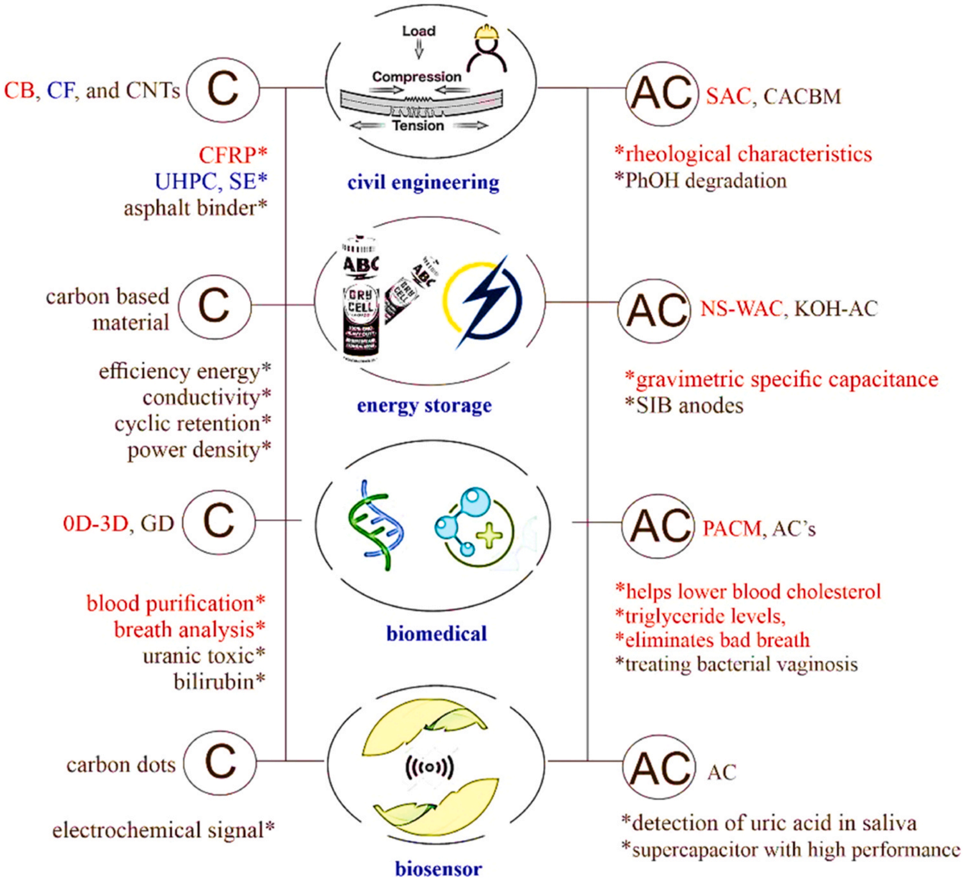

Fig. 9. Carbon and AC as multifunctional materials with different uses based on their compatible structure modifications.

of AC in biosensors has been explored for supercapacitors with high power density [166].

4. Conclusion and future direction

Carbon and AC offer enormous potential for a variety of environmental applications, particularly in addressing water pollution issues, where synthetic and natural sources provide myriad opportunities for the production of sustainable and cost-effective materials. It should be noted that in the 1906–2016 period, many isotherm equations were reported, whereby the chronological evolution of isotherm models can be seen by following the sequence:

(1906) Freundlich [167]→ (1910) Hill [168]→ (1918) Langmuir [169]→ (1925) Frumkin [170]→ Fowler, Ralph Howard. *Statistical thermodynamics*. CUP Archive, (1939) → (1942) Huggins [171]→ (1960) Dubinin [172]→ (1966) Anderson [173]→ (1974) Fritz [174]→ (1990) Baudu [175]→ (1990, 2016) [176] [177]→ (1995) Toth [178]→ (2016) Zou [179].

The potential of AC cannot be separated from its inherent adsorption properties such as surface deposition, and pore filling, as well as active sites supported by carbonyl, carboxyl, and hydrogen bonds. Performance improvements can be made through physio-chemical activation processes and utilizing RSM analysis, ANNs, isotherm models, and kinetic models to evaluate possible practical measures to optimize adsorption performance and advance applications. Highlighting the results of bibliometric analysis based on 35,245 articles has revealed active research efforts in countries such as China and India that are facing water pollution challenges, thus emphasizing the global interest in utilizing carbon and AC for remediation. Supported by the identified keyword network, it was found that ACs are predominantly used as adsorbents in combination with semiconductors as photocatalysts and further indicated specific focus areas within the research community. The data search process showed that Elsevier journals and environmental journals dominate the field of carbon and activated carbon (AC) research, with China and India being the most active countries. In addition, collaboration between countries is also evident, indicating knowledge exchange and joint efforts in addressing wastewater issues using carbon and AC. Finally, discussion on the implementation of carbon with various modifications and AC with porous structures have been presented as multifunctional materials in a number of fields.

CRediT authorship contribution statement

Mustafa Kavgaci: Resources. **Asnan Rinovian:** Software. **Dahlang Tahir:** Validation, Investigation. **Bualkar Abdullah:** Writing – review & editing, Writing – original draft. **M. I. Sayyed:** Writing – review & editing. **Rachid Masrour:** Supervision. **Venkata Siva Rama Prasad:** Formal analysis. **Heryanto Heryanto:** Writing – original draft, Visualization, Methodology, Investigation, Data curation, Conceptualization.

Declaration of Competing Interest

I have no relevant financial interests to disclose. I have the following potentially relevant financial interests: [there is no grant funding for honorarium or travel, this work is intended to support the completion of the author's Post-Doctoral studies. I have no relevant personal relationships to disclose.

Data Availability

Data will be made available on request.

Acknowledgment

The authors extend their gratitude for PDPU Program No. 00310/UN4.22/PT.01.03/2024, provided by Hasanuddin University, Makassar, Indonesia.

References

[1] Abdullah B, Tahir D, Heryanto H, Tang NFR, Rahmat R. Highly ordered structure and susceptibility to light absorption of ZnO/calcium phosphate (5%) to enhance the stability of charge diffusion as a methylene blue bond breaker. Phys Scr 2024;99:025901. https://doi.org/10.1088/1402-4896/ad17af.

[2] Elumalai P, Parthipan P, Gao X, Cui J, Kumar AS, Dhandapani P, Rajasekar A, Sarma H, Ganapathy NRV, Theerthagiri J, Min A, Choi MY. Impact of petroleum hydrocarbon and heavy metal pollution on coral reefs and mangroves: a review. Environ Chem Lett 2024. https://doi.org/10.1007/s10311-024-01728-0.

[3] Rahmat R, Heryanto H, Ilyas S, Fahri AN, Mutmainna I, Rahmi MH, Tahir D. The relation between structural, optical, and electronic properties of composite CuO/ZnO in supporting photocatalytic performance. Desalin Water Treat 2022;270:289–301. https://doi.org/10.5004/dwt.2022.28794.

[4] Syarifuddin S, Heryanto H, Suryani S, Tahir D. Biochar from diverse wastes: a comprehensive bibliometric analysis of heavymetal adsorption in wastewater. Desalin Water Treat 2024;317:100089. https://doi.org/10.1016/j.dwt.2024.100089.

[5] Chen D, Wang L, Ma Y, Yang W. Super-adsorbent material based on functional polymer particles with a multilevel porous structure. NPG Asia Mater 2016;8:e301–9. https://doi.org/10.1038/am.2016.117.

[6] Wang T, Pan R, Martins ML, Cui J, Huang Z, Thapaliya BP, Do-Thanh CL, Zhou M, Fan J, Yang Z, Chi M, Kobayashi T, Wu J, Mamontov E, Dai S. Machine-learning-assisted material discovery of oxygen-rich highly porous carbon active materials for aqueous supercapacitors. Nat Commun 2023;14. https://doi.org/10.1038/s41467-023-40282-1.

[7] Teimouri Z, Nanda S, Abatzoglou N, Dalai AK. Application of activated carbon in renewable energy conversion and storage systems: a review. Environ Chem Lett 2024. https://doi.org/10.1007/s10311-023-01690-3.

[8] Shi W, Li Z, Gong Z, Liang Z, Liu H, Han YC, Niu H, Song B, Chi X, Zhou J, Wang H, Xia BY, Yao Y, Tian ZQ. Transient and general synthesis of high-density and ultrasmall nanoparticles on two-dimensional porous carbon via coordinated carbothermal shock. Nat Commun 2023;14. https://doi.org/10.1038/s41467-023-38023-5.

[9] Grace AN, Sonar P, Bhardwaj P, Chakravorty A. Handbook of Porous Carbon Materials (eds.). Singapore: Springer Nature Singapore,; 2023. https://doi.org/10.1007/978-981-19-7188-4.

[10] Swain SK. Nanohybrid Materials for Water Purification (ed.). Singapore: Springer Nature Singapore,; 2022. https://doi.org/10.1007/978-981-19-2332-6.

[11] Novais GB, Dias MA, Santana AAM, Batista TC, Marques MN, Melo CR, Albuquerque RLC, Gomes MZ, Severino P, Souto EB, Cardoso JC. Isoflavones-functionalized single-walled and multi-walled carbon nanotubes: Synthesis and characterization of new nanoarchitetonics for biomedical uses. J Mol Struct 2023;1294:136351. https://doi.org/10.1016/j.molstruc.2023.136351.

[12] Neha G, Singh S, Kumar P, Malik Supreet. Recent trends and insights into carbon dots dispersed liquid crystal composites. J Mol Liq 2023;384:122225. https://doi.org/10.1016/j.molliq.2023.122225.

[13] Xu Z, Zhang C, Zhang C, Chen Z. Quantitative evaluation on phosphate adsorption by modified biochar: A meta-analysis. Process Saf Environ Prot 2023;177:42–51. https://doi.org/10.1016/j.psep.2023.06.063.

[14] Grich A, Bouzid T, Naboulsi A, Regti A, Tahiri AA, El Himri M, El Haddad M. Preparation of low-cost activated carbon from Doum fiber (Chamaerops humilis) for the removal of methylene blue: Optimization process by DOE/FFD design, characterization, and mechanism. J Mol Struct 2024;1295:136534. https://doi.org/10.1016/j.molstruc.2023.136534.

[15] Saleh TA, Sari A, Tuzen M. Optimization of parameters with experimental design for the adsorption of mercury using polyethylenimine modified-activated carbon. J Environ Chem Eng 2017;5:1079–88. https://doi.org/10.1016/j.jece.2017.01.032.

[16] Bonilla-Petriciolet A, Mendoza-Castillo DI, Reynel-Ávila HE. Adsorption Processes for Water Treatment and Purification (eds.). Cham: Springer International Publishing,; 2017. https://doi.org/10.1007/978-3-319-58136-1.

[17] Mukherjee A, Ruj B, Sadhukhan AK, Gupta P, Chakrabortty S, Chatterjee R, Bishayee B. Eco-synthesis, characterization and application of waste plastics pyrolysis char in arsenic removal from contaminated water: An integrated circular framework with parametric response surface methodology optimization-cum-artificial neural network model. J Environ Chem Eng 2024;12:111824. https://doi.org/10.1016/j.jece.2023.111824.

[18] Zhao R, Yang Z, Zheng H, Wu Y, Liu F, Wu Z, Li L, Chen F, Song S, Zhu J, Zhang W, Huang H, Xu M, Sheng K, Yin Q, Pei J, Li G, Zhang Y, Zhao M, Shi L. A framework for the general design and computation of hybrid neural networks. Nat Commun 2022;13. https://doi.org/10.1038/s41467-022-30964-7.

[19] Osman AI, El-Monaem EMA, Elgarahy AM, Aniagor CO, Hosny M, Farghali M, Rashad E, Ejimofor MI, López-Maldonado EA, Ihara I, Yap PS, Rooney DW, Eltaweil AS. Methods to prepare biosorbents and magnetic sorbents for water treatment: a review. Springer International Publishing,; 2023. https://doi.org/10.1007/s10311-023-01603-4.

[20] Heryanto H, Tahir D. Enhancing Photocatalyst Performance of Magnetic Surfaces Covered by Carbon Clouds for Textile Dye Degradation. Arab J Sci Eng 2023. https://doi.org/10.1007/s13369-023-08532-y.

[21] Nath H, Saikia A, Goutam PJ, Saikia BK, Saikia N. Removal of methylene blue from water using okra (Abelmoschus esculentus L.) mucilage modified biochar. Bioresour Technol Rep 2021;14:100689. https://doi.org/10.1016/j.biteb.2021.100689.

[22] Isaac R, Siddiqui S. Adsorption of divalent copper from aqueous solution by magnesium chloride co-doped Cicer arietinum husk biochar: Isotherm, kinetics, thermodynamic studies and response surface methodology. Bioresour Technol Rep 2022;18:101004. https://doi.org/10.1016/j.biteb.2022.101004.

[23] Rahimi E, Sajednia G, Baghdadi M, Karbassi A. Catalytic chemical reduction of nitrate from simulated groundwater using hydrogen radical produced on the surface of palladium catalyst supported on the magnetic alumina nanoparticles. J Environ Chem Eng 2018;6:5249–58. https://doi.org/10.1016/j.jece.2018.08.026.

[24] Song Q, Li M, Li J, Zhang S, Yang L, Chen X, Meng F, Liu X. Simultaneous electrocatalytic removal of inorganic nitrogen compounds in groundwater: Modeling and mechanistic studies. Chem Eng J 2022;430:133152. https://doi.org/10.1016/j.cej.2021.133152.

[25] Danovaro R, Cocozza di Montanara A, Corinaldesi C, Dell'Anno A, Illuminati S, Willis TJ, Gambi C. Bioaccumulation and biomagnification of heavy metals in marine micro-predators. Commun Biol 2023;6. https://doi.org/10.1038/s42003-023-05539-x.

[26] Alardhi SM, Salih HG, Ali NS, Khalbas AH, Salih IK, Saady NMC, Zendehboudi S, Albayati TM, Harharah HN. Olive stone as an eco-friendly bio-adsorbent for elimination of methylene blue dye from industrial wastewater. Sci Rep 2023;13:1–14. https://doi.org/10.1038/s41598-023-47319-x.

[27] Magnier L, Cossard G, Martin V, Pascal C, Roche V, Sibert E, Shchedrina I, Bousquet R, Parry V, Chatenet M. Fe–Ni-based alloys as highly active and low-cost oxygen evolution reaction catalyst in alkaline media. Nat Mater 2024;23:252–61. https://doi.org/10.1038/s41563-023-01744-5.

[28] Ahmed A, Usman M, Liu QY, Shen YQ, Yu B, Cong HL. Plant mediated synthesis of copper nanoparticles by using Camelia sinensis leaves extract and their applications in dye degradation. Ferroelectrics 2019;549:61–9. https://doi.org/10.1080/00150193.2019.1592544.

[29] Zhang Y, Kirk C, Robertson N. Nitrogen Doping and Carbon Coating Affects Substrate Selectivity of TiO2 Photocatalytic Organic Pollutant Degradation. ChemPhysChem 2020;21:2643–50. https://doi.org/10.1002/cphc.202000492.

[30] Moosavi S, Li RYM, Lai CW, Yusof Y, Gan S, Akbarzadeh O, Chowhury ZZ, Yue XG, Johan MR. Methylene blue dye photocatalytic degradation over synthesised fe3 o4 /ac/tio2 nano-catalyst: Degradation and reusability studies. Nanomaterials 2020;10:1–15. https://doi.org/10.3390/nano10122360.

[31] Nieto-Delgado C, Terrones M, Rangel-Mendez JR. Development of highly microporous activated carbon from the alcoholic beverage industry organic by-products. Biomass– Bioenergy 2011;35:103–12. https://doi.org/10.1016/j.biombioe.2010.08.025.

[32] Qiu C, Jiang L, Gao Y, Sheng L. Effects of oxygen-containing functional groups on carbon materials in supercapacitors: A review. Mater Des 2023;230:111952. https://doi.org/10.1016/j.matdes.2023.111952.

[33] Basta AH, Fierro V, El-Saied H, Celzard A. 2-Steps KOH activation of rice straw: An efficient method for preparing high-performance activated carbons. Bioresour Technol 2009;100:3941–7. https://doi.org/10.1016/j.biortech.2009.02.028.

[34] Yi H, Nakabayashi K, Yoon SH, Miyawaki J. Pressurized physical activation: A simple production method for activated carbon with a highly developed pore structure. Carbon N Y 2021;183:735–42. https://doi.org/10.1016/j.carbon.2021.07.061.

[35] Zhao Q, Zhang S, Huang X, Tan Y, Zhang Y, Chen Y. Coffee charcoal as a green catalyst for oxidative dehydrogenation. Chem Eng J 2024;479:147784. https://doi.org/10.1016/j.cej.2023.147784.

[36] Mariana M, Mistar EM, Syabriyana M, Zulkipli AS, Aswita D, Alfatah T. Properties and adsorptive performance of candlenut shell and its porous charcoals for aqueous mercury(II) removal. Bioresour Technol Rep 2022;19:101182. https://doi.org/10.1016/j.biteb.2022.101182.

[37] Pak T, Gomari KE, Bose S, Tonon T, Hughes D, Gronnow M, Macquarrie D. Biochar from brown algae: Production, activation, and characterisation. Bioresour Technol Rep 2023;24:101688. https://doi.org/10.1016/j.biteb.2023.101688.

[38] Bukar UA, Sayeed MS, Razak SFA, Yogarayan S, Amodu OA, Mahmood RAR. A method for analyzing text using VOSviewer. MethodsX 2023;11:102339. https://doi.org/10.1016/j.mex.2023.102339.

[39] Teplitskiy M, Duede E, Menietti M, Lakhani KR. How status of research papers affects the way they are read and cited. Res Policy 2022;51:104484. https://doi.org/10.1016/j.respol.2022.104484.

[40] Hammad WA, Darweesh MA, Zouli N, Osman SM, Eweida B, Amr MHA. Adsorption of cationic dye onto Raphanus seeds: optimization, adsorption kinetics, thermodynamic studies. Sci Rep 2024;14:17827. https://doi.org/10.1038/s41598-024-66761-z.

[41] Hashem HM, El-Maghrabey M, El-Shaheny R. Inclusive study of peanut shells derived activated carbon as an adsorbent for removal of lead and methylene blue from water. Sci Rep 2024;14:13515. https://doi.org/10.1038/s41598-024-63585-9.

[42] Chauhan A, Chandola S, Aneja R, Kumar Saini V. Exploring the adsorptive potential of chemically activated Nanoporous carbons derived from invasive goat weed for treatment of hospital wastewater. Mater Lett 2024;374:137182. https://doi.org/10.1016/j.matlet.2024.137182.

[43] Lingamdinne LP, Angaru GKR, Pal CA, Koduru JR, Karri RR, Mubarak NM, Chang Y-Y. Insights into kinetics, thermodynamics, and mechanisms of chemically activated sunflower stem biochar for removal of phenol and bisphenol-A from wastewater. Sci Rep 2024;14:4267. https://doi.org/10.1038/s41598-024-54907-y.

[44] Naribi Z, Nechchadi B, Mouratib R, Ghazzaf H, Salhi A, El Krati M, Tahiri S. Activated carbon from hydrothermal carbonization of ice cream factory wastewater with H3PO4 activation. Synthesis, characterisation and adsorption properties. Sustain Chem Pharm 2024;41:101697. https://doi.org/10.1016/j.scp.2024.101697.

[45] Hao YS, Othman N, Zaini MAA. Waste newspaper as cellulose resource of activated carbon by sodium salts for methylene blue and congo red removal. Int J Biol Macromol 2024;277:134353. https://doi.org/10.1016/j.ijbiomac.2024.134353.

[46] Naribi Z, Nechchadi B, Mouratib R, Ghazzaf H, Salhi A, El Krati M, Tahiri S. Activated carbon from hydrothermal carbonization of ice cream factory wastewater with H3PO4 activation. Synthesis, characterisation and adsorption properties. Sustain Chem Pharm 2024;41:101697. https://doi.org/10.1016/j.scp.2024.101697.

[47] Rehan K, Malaibari Z, Atieh M, Hussain I, Abu-Saud B. A highly efficient modified nano-activated carbon adsorbent for separation of ammonia from water: Experimental and kinetics elucidations. Chemosphere 2024;364:143048. https://doi.org/10.1016/j.chemosphere.2024.143048.

[48] Zhu S, Xu J, Xie J, Zhang Z, Ding Q, Chen K. Ultrafast dyeing wastewater purification by high-performance and reusable lignin-derived activated porous carbon filter. Sep Purif Technol 2024;349:127672. https://doi.org/10.1016/j.seppur.2024.127672.

[49] Hammad WA, Darweesh MA, Zouli N, Osman SM, Eweida B, Amr MHA. Adsorption of cationic dye onto Raphanus seeds: optimization, adsorption kinetics, thermodynamic studies. Sci Rep 2024;14:17827. https://doi.org/10.1038/s41598-024-66761-z.

[50] Mustafa D, Ibrahim B, Erten A. Adsorptive removal of anticarcinogen pazopanib from aqueous solutions using activated carbon: isotherm, kinetic and thermodynamic studies. Sci Rep 2024;14:17765. https://doi.org/10.1038/s41598-024-68666-3.

[51] Mkilima T, Zharkenov Y, Abduova A, Sarypbekova N, Kudaibergenov N, Sakanov K, Zhukenova G, Omarov Z, Sultanbekova P, Kenzhaliyeva G. Utilization of banana peel-derived activated carbon for the removal of heavy metals from industrial wastewater. Case Stud Chem Environ Eng 2024;10:100791. https://doi.org/10.1016/j.cscee.2024.100791.

[52] Hashem HM, El-Maghrabey M, El-Shaheny R. Inclusive study of peanut shells derived activated carbon as an adsorbent for removal of lead and methylene blue from water. Sci Rep 2024;14:13515. https://doi.org/10.1038/s41598-024-63585-9.

[53] Sayed NSM, Ahmed ASA, Abdallah MH, Gouda GA. ZnO@ activated carbon derived from wood sawdust as adsorbent for removal of methyl red and methyl orange from aqueous solutions. Sci Rep 2024;14:5384. https://doi.org/10.1038/s41598-024-55158-7.

[54] Amir D, Nasaruddin RR, Yousefi M, Mastuli MS, Sulaiman S, Alam MdZ, Engliman NS. Investigating the synthesis parameters of durian skin-based activated carbon and the effects of silver nanocatalysts on its recyclability in methylene blue removal. Discov Nano 2024;19:32. https://doi.org/10.1186/s11671-024-03974-1.

[55] Lingamdinne LP, Angaru GKR, Pal CA, Koduru JR, Karri RR, Mubarak NM, Chang Y-Y. Insights into kinetics, thermodynamics, and mechanisms of chemically activated sunflower stem biochar for removal of phenol and bisphenol-A from wastewater. Sci Rep 2024;14:4267. https://doi.org/10.1038/s41598-024-54907-y.

[56] El Jery A, Alawamleh HSK, Sami MH, Abbas HA, Sammen SSh, Ahsan A, Imteaz MA, Shanableh A, Shafiquzzaman Md, Osman H, Al-Ansari N. Isotherms, kinetics and thermodynamic mechanism of methylene blue dye adsorption on synthesized activated carbon. Sci Rep 2024;14:970. https://doi.org/10.1038/s41598-023-50937-0.

[57] Chauhan A, Chandola S, Aneja R, Kumar Saini V. Exploring the adsorptive potential of chemically activated Nanoporous carbons derived from invasive goat weed for treatment of hospital wastewater. Mater Lett 2024;374:137182. https://doi.org/10.1016/j.matlet.2024.137182.

[58] Tang X, Yao M, Li J. Boric acid-modified activated carbon for glycerol removal from high-salt wastewater. Appl Surf Sci 2024;670:160660. https://doi.org/10.1016/j.apsusc.2024.160660.

[59] Hao YS, Othman N, Zaini MAA. Waste newspaper as cellulose resource of activated carbon by sodium salts for methylene blue and congo red removal. Int J Biol Macromol 2024;277:134353. https://doi.org/10.1016/j.ijbiomac.2024.134353.

[60] Mahmoud R, Mahgoub SM, Ashraf AM, Allam AA, Alawam AS, Rudayni HA, Moaty SA. Activated carbon alginate as adsorbent for simultaneous removal of almotriptan and paracetamol from binary solutions. Sustain Chem Pharm 2024;41:101708. https://doi.org/10.1016/j.scp.2024.101708.

[61] Naribi Z, Nechchadi B, Mouratib R, Ghazzaf H, Salhi A, El Krati M, Tahiri S. Activated carbon from hydrothermal carbonization of ice cream factory wastewater with H3PO4 activation. Synthesis, characterisation and adsorption properties. Sustain Chem Pharm 2024;41:101697. https://doi.org/10.1016/j.scp.2024.101697.

[62] He L, Qi X, Wei W, Zhang X, Wang J, Gao Z. Biomass-activated carbon-based superhydrophobic sponge with photothermal properties for adsorptive separation of waste oil. J Hazard Mater 2024;477:135222. https://doi.org/10.1016/j.jhazmat.2024.135222.

[63] Fakoya TO, Oyekunle JAO, Adekunle AS, Oyinloye AJ, Ejidike IP. Removal of hexachlorocyclohexane isomers from wastewater using activated carbon from Musa paradisiaca peel: Adsorption isotherms, kinetic, and thermodynamic studies. Chem Thermodyn Therm Anal 2024;15:100140. https://doi.org/10.1016/j.ctta.2024.100140.

[64] Zhao H, Li J, Li S, Jiang Y, Du L. Evaluation and optimization of six adsorbents for removal of tetracycline from swine wastewater: Experiments and response surface analysis. J Environ Manag 2024;368:122170. https://doi.org/10.1016/j.jenvman.2024.122170.

[65] Rehan K, Malaibari Z, Atieh M, Hussain I, Abu-Saud B. A highly efficient modified nano-activated carbon adsorbent for separation of ammonia from water: Experimental and kinetics elucidations. Chemosphere 2024;364:143048. https://doi.org/10.1016/j.chemosphere.2024.143048.

[66] Al-sareji OJ, Grmasha RA, Meiczinger M, Al-Juboori RA, Jakab M, Boros A, Majdi HSh, Miskolczi N, Hashim KS. A novel two stages chemical activation of pinewood waste for removing organic micropollutants from water and wastewater. Chemosphere 2024;363:142974. https://doi.org/10.1016/j.chemosphere.2024.142974.

[67] Enad HY. An experiment on using activated carbon to remove direct dyes from wastewater collected from the textile dyeing industry. Eng Res Express 2024;6:035105. https://doi.org/10.1088/2631-8695/ad62b3.

[68] Grzybek J, Kubů M, Roth WJ, Gil B, Čejka J, Kasneryk V. Structural transformation and chemical modifications of the unusual layered zeolite MWW form SSZ-70. Catal Today 2020;354:133–40. https://doi.org/10.1016/j.cattod.2019.03.006.

[69] Ma X, Zhang Z, Wu H, Li J, Yang L. Adsorption of Volatile Organic Compounds at Medium-High Temperature Conditions by Activated Carbons. Energy Fuels 2020;34:3679–90. https://doi.org/10.1021/acs.energyfuels.9b03292.

[70] Yakout SM, Sharaf El-Deen G. Characterization of activated carbon prepared by phosphoric acid activation of olive stones. Arab J Chem 2016;9:S1155–62. https://doi.org/10.1016/j.arabjc.2011.12.002.

[71] Masoud N, Bordanaba-Florit G, van Haasterecht T, Bitter JH. Effect of Support Surface Properties on CO_2 Capture from Air by Carbon-Supported Potassium Carbonate. Ind Eng Chem Res 2021;60:13749–55. https://doi.org/10.1021/acs.iecr.1c01229.

[72] Ozdemir I, Şahin M, Orhan R, Erdem M. Preparation and characterization of activated carbon from grape stalk by zinc chloride activation. Fuel Process Technol 2014;125:200–6. https://doi.org/10.1016/j.fuproc.2014.04.002.

[73] El-Desouky MG, Alayyafi AA, Al-Hazmi GAAM, El-Bindary AA. Effect of metal organic framework alginate aerogel composite sponge on adsorption of tartrazine from aqueous solutions: Adsorption models, thermodynamics and optimization via Box-Behnken design. J Mol Liq 2024;399:124392. https://doi.org/10.1016/j.molliq.2024.124392.

[74] Nassef HM, Al-Hazmi GAAM, Alayyafi AA, El-Desouky MG, El-Bindary AA. Synthesis and characterization of new composite sponge combining of metal-organic framework and chitosan for the elimination of Pb(II), Cu(II) and Cd(II) ions from aqueous solutions: Batch adsorption and optimization using Box-Behnken design. J Mol Liq 2024;394:123741. https://doi.org/10.1016/j.molliq.2023.123741.

[75] Mohammed Alsuhaibani A, Alayyafi AA, Albedair LA, El-Desouky MG, El-Bindary AA. Synthesis and characterization of metal–organic frameworks based on thorium for the effective removal of 2,4-dichlorophenylacetic pesticide from water: Batch adsorption and Box-Behnken Design optimization, and evaluation of reusability. J Mol Liq 2024;398:124252. https://doi.org/10.1016/j.molliq.2024.124252.

[76] Scholze F, Henneken H, Kuschnerus P, Rabus H, Richter M, Ulm G. Determination of the electron-hole pair creation energy for semiconductors from the spectral responsivity of photodiodes. Nucl Instrum Methods Phys Res A 2000;439:208–15. https://doi.org/10.1016/S0168-9002(99)00937-7.

[77] Al-Hazmi GAA, El-Zahhar AA, El-Desouky MG, El-Bindary MA, El-Bindary AA. Adsorption of industrial dye onto a zirconium metal-organic framework: synthesis, characterization, kinetics, thermodynamics, and DFT calculations. J Coord Chem 2022;75:1203–29. https://doi.org/10.1080/00958972.2022.2114349.

[78] Almahri A, Abou-Melha KS, Katouah HA, Al-bonayan AM, Saad FA, El-Desouky MG, El-Bindary AA. Adsorption and removal of the harmful pesticide 2,4-dichlorophenylacetic acid from an aqueous environment via coffee waste biochar: Synthesis, characterization, adsorption study and optimization via Box-Behnken design. J Mol Struct 2023;1293:136238. https://doi.org/10.1016/j.molstruc.2023.136238.

[79] Kocha SS. Electrochemical Degradation: Electrocatalyst and Support Durability. Elsevier Inc.,; 2011. https://doi.org/10.1016/B978-0-12-386936-4.10003-X.

[80] Yang HJ, Kim J, Bae JH. Selectivity of Electrochemical Reactions Based on Adsorption at Nanoporous Electrodes. Anal Chem 2023;95:16216–24. https://doi.org/10.1021/acs.analchem.3c02991.

[81] Zhou K, Chen J, Wang T, Su Y, Qiao L, Yan Y. Effect of surface energy on protein adsorption behaviours of treated CoCrMo alloy surfaces. Appl Surf Sci 2020;520:146354. https://doi.org/10.1016/j.apsusc.2020.146354.

[82] Serafin J, Ouzzine M, Xing C, El Ouahabi H, Kamińska A, Sreńscek-Nazzal J. Activated carbons from the Amazonian biomass andiroba shells applied as a CO_2 adsorbent and a cheap semiconductor material. J CO_2 Util 2022;62:102071. https://doi.org/10.1016/j.jcou.2022.102071.

[83] Yue Z, Vakili A. Activated carbon–carbon composites made of pitch-based carbon fibers and phenolic resin for use of adsorbents. J Mater Sci 2017;52:12913–21. https://doi.org/10.1007/s10853-017-1389-7.

[84] Kumari S, Verma A, Sharma P, Agarwal S, Rajput VD, Minkina T, Rajput P, Singh SP, Garg MC. Introducing machine learning model to response surface methodology for biosorption of methylene blue dye using Triticum aestivum biomass. Sci Rep 2023;13:1–17. https://doi.org/10.1038/s41598-023-35645-z.

[85] Wang R, Yang K, Wong C, Aguirre-Villegas H, Larson R, Brushett F, Qin M, Jin S. Electrochemical ammonia recovery and co-production of chemicals from manure wastewater. Nat Sustain 2023;7:179–90. https://doi.org/10.1038/s41893-023-01252-z.

[86] T.O. Ozcelik, M. Cetinkaya, B. Sarici, D. Bozdag, E. Altintig, Optimization of Methylene Blue Adsorption on Olive Seed Activated Carbon Using Response Surface Methodology (RSM) Modeling-Artificial Neural Network, in: 2024: pp. 710–721. https://doi.org/10.1007/978–981-99–6062-0_67.

[87] Godvin Sharmila V, Kumar Tyagi V, Varjani S, Rajesh Banu J. A review on the lignocellulosic derived biochar-based catalyst in wastewater remediation: Advanced treatment technologies and machine learning tools. Bioresour Technol 2023;387:129587. https://doi.org/10.1016/j.biortech.2023.129587.

[88] Ghaedi AM, Vafaei A. Applications of artificial neural networks for adsorption removal of dyes from aqueous solution: A review. Adv Colloid Interface Sci 2017; 245:20–39. https://doi.org/10.1016/j.cis.2017.04.015.

[89] Heryanto H, Ardiansyah A, Rahmat R, Tahir D. Science Mapping Analysis of Density Functional Theory (DFT) for Material Design: A Review. JOM 2024. https://doi.org/10.1007/s11837-024-06644-w.

[90] Hanasaki K, Ali ZA, Choi M, Del Ben M, Wong BM. Implementation of real-time TDDFT for periodic systems in the open-source PySCF software package. J Comput Chem 2022. https://doi.org/10.1002/jcc.27058.

[91] Jamshed W, Eid MR, Al-Hossainy AF, Raizah Z, Tag El Din ESM, Sajid T. Experimental and TDDFT materials simulation of thermal characteristics and entropy optimized of Williamson Cu-methanol and Al2O3-methanol nanofluid flowing through solar collector. Sci Rep 2022;12. https://doi.org/10.1038/s41598-022-23025-y.

[92] Ganji MD, Mirzaei Sh, Dalirandeh Z. Molecular origin of drug release by water boiling inside carbon nanotubes from reactive molecular dynamics simulation and DFT perspectives. Sci Rep 2017;7:4669. https://doi.org/10.1038/s41598-017-04981-2.

[93] Nemati-Kande E, Pourasadi A, Aghababaei F, Baranipour S, Mehdizadeh A, Sardroodi JJ. Quantum DFT methods to explore the interaction of 1-Adamantylamine with pristine, and P, As, Al, and Ga doped BN nanotubes. Sci Rep 2022; 12:19972. https://doi.org/10.1038/s41598-022-24200-x.

[94] Gupta SV, Kulkarni VV, Ahmaruzzaman Md. Bandgap engineering approach for designing CuO/Mn3O4/CeO2 heterojunction as a novel photocatalyst for AOP-assisted degradation of Malachite green dye. Sci Rep 2023;13:3009. https://doi.org/10.1038/s41598-023-30096-y.

[95] Kitchamsetti N, Ramteke MS, Rondiya SR, Mulani SR, Patil MS, Cross RW, Dzade NY, Devan RS. DFT and experimental investigations on the photocatalytic activities of NiO nanobelts for removal of organic pollutants. J Alloy Compd 2021;855:157337. https://doi.org/10.1016/j.jallcom.2020.157337.

[96] Gan Z, Yin J, Xu X, Cheng Y, Yu T. Nanostructure and Advanced Energy Storage: Elaborate Material Designs Lead to High-Rate Pseudocapacitive Ion Storage. ACS Nano 2022;16:5131–52. https://doi.org/10.1021/acsnano.2c00557.

[97] Gan Z, Xia L, Yin J, Gao Y, Feng X, Meng G, Cheng Y, Xu X. Simulation-Assisted Modularized Material Design Protocol Enables MoS $_2$ to Realize Superior Zinc-Ion Storage. ACS Appl Energy Mater 2022;5:15452–62. https://doi.org/10.1021/acsaem.2c03046.

[98] Pernigoni L, Lafont U, Grande AM. Self-healing materials for space applications: overview of present development and major limitations. CEAS Space J 2021;13: 341–52. https://doi.org/10.1007/s12567-021-00365-5.

[99] Wei M, Marrakchi F, Yuan C, Cheng X, Jiang D, Zafar FF, Fu Y, Wang S. Adsorption modeling, thermodynamics, and DFT simulation of tetracycline onto mesoporous and high-surface-area NaOH-activated macroalgae carbon. J Hazard Mater 2022;425:127887. https://doi.org/10.1016/j.jhazmat.2021.127887.

[100] Wang S, Zhao S, Cheng X, Qian L, Barati B, Gong X, Cao B, Yuan C. Study on two-step hydrothermal liquefaction of macroalgae for improving bio-oil. Bioresour Technol 2021;319:124176. https://doi.org/10.1016/j.biortech.2020.124176.

[101] Khnifira M, Mahsoune A, Belghiti ME, Khamar L, Sadiq M, Abdennouri M, Barka N. Combined DFT and MD simulation approach for the study of SO2 and CO_2 adsorption on graphite (111) surface in aqueous medium. Curr Res Green Sustain Chem 2021;4:100085. https://doi.org/10.1016/j.crgsc.2021.100085.

[102] Sun H. COMPASS: An ab Initio Force-Field Optimized for Condensed-Phase ApplicationsOverview with Details on Alkane and Benzene Compounds. J Phys Chem B 1998;102:7338–64. https://doi.org/10.1021/jp980939v.

[103] Al-Ghouti MA. D.A. Da'ana, Guidelines for the use and interpretation of adsorption isotherm models: A review. J Hazard Mater 2020;393:122383. https://doi.org/10.1016/j.jhazmat.2020.122383.

[104] Lima EC, Hosseini-Bandegharaei A, Moreno-Piraján JC, Anastopoulos I. A critical review of the estimation of the thermodynamic parameters on adsorption equilibria. Wrong use of equilibrium constant in the Van't Hoof equation for calculation of thermodynamic parameters of adsorption. J Mol Liq 2019;273: 425–34. https://doi.org/10.1016/j.molliq.2018.10.048.

[105] Tran HN, You SJ, Hosseini-Bandegharaei A, Chao HP. Mistakes and inconsistencies regarding adsorption of contaminants from aqueous solutions: A critical review. Water Res 2017;120:88–116. https://doi.org/10.1016/j.watres.2017.04.014.

[106] Hansen JB. Kinetics of Ammonia Synthesis and Decomposition on Heterogeneous Catalysts, in: Ammonia. Berlin, Heidelberg: Springer Berlin Heidelberg,; 1995. p. 149–90. https://doi.org/10.1007/978-3-642-79197-0_4.

[107] Halsey G. Physical adsorption on non-uniform surfaces. J Chem Phys 1948;16: 931–7. https://doi.org/10.1063/1.1746689.

[108] Harkins WD, Jura G. Surfaces of Solids. XIII. A Vapor Adsorption of a Monolayer Area, and the Areas Occupied be Nitrogen and other Molecules on the Surface of a Solid. J Am Chem Soc 1944;66:1366–73.

[109] Jovanović DS. Physical adsorption of gases. Kolloid-Z Z Für Polym 1969;235: 1214–25. https://doi.org/10.1007/bf01542531.

[110] Sandoval DR, Yan W, Michelsen ML, Stenby EH. Influence of Adsorption and Capillary Pressure on Phase Equilibria inside Shale Reservoirs. Energy Fuels 2018; 32:2819–33. https://doi.org/10.1021/acs.energyfuels.7b03274.

[111] Liu L, Luo XB, Ding L, Luo SL. Application of Nanotechnology in the Removal of Heavy Metal From Water. Elsevier Inc.,; 2018. https://doi.org/10.1016/B978-0-12-814837-2.00004-4.

[112] Behloul S, Hamitouche AE, Haffas M, Boudjemaa A, Benammar S, Sehailia M, Meziane T, Bachari K. Removal of methyl violet dye by a low-cost waste (Ajuga Pseudo-Iva): Kinetic and equilibrium isotherm study. Can J Chem Eng 2018;96: 2282–91. https://doi.org/10.1002/cjce.23313.

[113] Chu KH. Revisiting the Temkin Isotherm: Dimensional Inconsistency and Approximate Forms. Ind Eng Chem Res 2021;60:13140–7. https://doi.org/10.1021/acs.iecr.1c01788.

[114] Wang J, Guo X. Rethinking of the intraparticle diffusion adsorption kinetics model: Interpretation, solving methods and applications. Chemosphere 2022;309: 136732. https://doi.org/10.1016/j.chemosphere.2022.136732.

[115] Ayawei N, Ebelegi AN, Wankasi D. Modelling and Interpretation of Adsorption Isotherms. J Chem 2017;2017. https://doi.org/10.1155/2017/3039817.

[116] Mozaffari Majd M, Kordzadeh-Kermani V, Ghalandari V, Askari A, Sillanpää M. Adsorption isotherm models: A comprehensive and systematic review (2010−2020). Sci Total Environ 2022;812:151334. https://doi.org/10.1016/j.scitotenv.2021.151334.

[117] Kalam S, Abu-Khamsin SA, Kamal MS, Patil S. Surfactant Adsorption Isotherms: A Review. ACS Omega 2021;6:32342–8. https://doi.org/10.1021/acsomega.1c04661.

[118] Dos Santos Escobar O, Ferraz De Azevedo C, Swarowsky A, Adebayo MA, Schadeck Netto M, Machado Machado F. Utilization of different parts of Moringa oleifera Lam. seeds as biosorbents to remove Acid Blue 9 synthetic dye. J Environ Chem Eng 2021;9. https://doi.org/10.1016/j.jece.2021.105553.

[119] Vijayan DS, Sivasuriyan A, Devarajan P, Stefańska A, Wodzyński E, Koda. Carbon Fibre-Reinforced Polymer (CFRP) Composites in Civil Engineering Application—A Comprehensive Review. Buildings 2023;13:1509. https://doi.org/10.3390/buildings13061509.

[120] Bahuguna A. Sustainable Construction Materials for Civil Engineering Projects. Math Stat Eng Appl 2021;70:637–45. https://doi.org/10.17762/msea.v70i1.2518.

[121] Wang J, Xie J, Liu Y. Sustainable Cementitious Materials for Civil and Transportation Engineering. Materials 2023;16:6290. https://doi.org/10.3390/ma16186290.

[122] Khan A-R, Nasir R, Fareed S. Simulation of Reinforced Concrete Columns Strengthened with CFRP Wraps. Int J Civ Eng 2023;21:299–313. https://doi.org/10.1007/s40999-022-00768-3.

[123] Vijayan DS, Sivasuriyan A, Devarajan P, Stefańska A, Wodzyński E, Koda. Carbon Fibre-Reinforced Polymer (CFRP) Composites in Civil Engineering Application—A Comprehensive Review. Buildings 2023;13:1509. https://doi.org/10.3390/buildings13061509.

[124] Jung M, Lee Y, Hong S-G, Moon J. Carbon nanotubes (CNTs) in ultra-high performance concrete (UHPC): Dispersion, mechanical properties, and electromagnetic interference (EMI) shielding effectiveness (SE). Cem Concr Res 2020;131:106017. https://doi.org/10.1016/j.cemconres.2020.106017.

[125] Rafi J, Kamal M, Ahmad N, Hafeez M, Faizan ul Haq M, Aamara Asif S, Shabbir F, Bilal Ahmed Zaidi S. Performance Evaluation of Carbon Black Nano-Particle Reinforced Asphalt Mixture. Appl Sci 2018;8:1114. https://doi.org/10.3390/app8071114.

[126] Lekkam M, Benmounah A, Kadri E-H, Soualhi H, Kaci A. Influence of saturated activated carbon on the rheological and mechanical properties of cementitious materials. Constr Build Mater 2019;198:411–22. https://doi.org/10.1016/j.conbuildmat.2018.11.257.

[127] Annamalai S, Septian A, Choi J, Shin WS. Remediation of phenol contaminated soil using persulfate activated by ball-milled colloidal activated carbon. J Environ Manag 2022;310:114709. https://doi.org/10.1016/j.jenvman.2022.114709.

[128] Shen S, Chen Y, Zhou J, Zhang H, Xia X, Yang Y, Zhang Y, Noori A, Mousavi MF, Chen M, Xia Y, Zhang W. Microbe-Mediated Biosynthesis of Multidimensional Carbon-Based Materials for Energy Storage Applications. Adv Energy Mater 2023; 13. https://doi.org/10.1002/aenm.202204259.

[129] Hu W, Zheng M, Xu B, Wei Y, Zhu W, Li Q, Pang H. Design of hollow carbon-based materials derived from metal–organic frameworks for electrocatalysis and electrochemical energy storage. J Mater Chem A Mater 2021;9:3880–917. https://doi.org/10.1039/D0TA10666F.

[130] Wang J, Kaskel S. KOH activation of carbon-based materials for energy storage. J Mater Chem 2012;22:23710. https://doi.org/10.1039/c2jm34066f.

[131] Sahoo PK, Kumar N, Jena A, Mishra S, Lee C-P, Lee S-Y, Park S-J. Recent progress in graphene and its derived hybrid materials for high-performance supercapacitor electrode applications. RSC Adv 2024;14:1284–303. https://doi.org/10.1039/D3RA06904D.

[132] Jia H, Su P, Fan J, Guo T, Zhang Y, Miao L, Wan L, Yang P, Liu M-C. Constructing Co N C coordination in Co9S8 embedded N,S-codoped carbon nanotube as an advanced electrode for supercapacitor and Na-ion battery. J Colloid Interface Sci 2024;659:974–83. https://doi.org/10.1016/j.jcis.2024.01.062.

[133] Anand S, Wasi Ahmad Md, Syed A, Bahkali AH, Verma M, Hye Kim B, Choudhury A. Walnut shell derived N, S co-doped activated carbon for solid-state symmetry supercapacitor device. J Ind Eng Chem 2024;129:309–20. https://doi.org/10.1016/j.jiec.2023.08.045.

[134] Jeon I, Kim T, Seo J, Jeong I-K, Lee JH, Park M, Park Y, Yang D, Cho CR. Enhanced electrochemical performance and interdiffusion behavior of sodium ions in onion-derived freeze-dried and KOH-activated carbon for sodium-ion battery anodes. Appl Surf Sci 2024;648:159023. https://doi.org/10.1016/j.apsusc.2023.159023.

[135] Chaudhary P, Bansal S, Sharma BB, Saini S, Joshi A. Waste biomass-derived activated carbons for various energy storage device applications: A review. J Energy Storage 2024;78:109996. https://doi.org/10.1016/j.est.2023.109996.

[136] Si H, Wang Q, Guo Y, Zhao Y, Li H, Li S, Wang S, Zhu B. Functionalized monolithic columns: Recent advancements and their applications for high-efficiency separation and enrichment in food and medicine. Front Chem 2022;10. https://doi.org/10.3389/fchem.2022.951649.

[137] Kato S, Otake K, Chen H, Akpinar I, Buru CT, Islamoglu T, Snurr RQ, Farha OK. Zirconium-Based Metal–Organic Frameworks for the Removal of Protein-Bound Uremic Toxin from Human Serum Albumin. J Am Chem Soc 2019;141:2568–76. https://doi.org/10.1021/jacs.8b12525.

[138] Ujjain SK, Bagusetty A, Matsuda Y, Tanaka H, Ahuja P, de Tomas C, Sakai M, Vallejos-Burgos F, Futamura R, Suarez-Martinez I, Matsukata M, Kodama A, Garberoglio G, Gogotsi Y, Karl Johnson J, Kaneko K. Adsorption separation of heavier isotope gases in subnanometer carbon pores. Nat Commun 2021;12:546. https://doi.org/10.1038/s41467-020-20744-6.

[139] Molinero-Fernández Á, Arruza L, López MÁ, Escarpa A. On-the-fly rapid immunoassay for neonatal sepsis diagnosis: C-reactive protein accurate determination using magnetic graphene-based micromotors. Biosens Bioelectron 2020;158:112156. https://doi.org/10.1016/j.bios.2020.112156.

[140] Panwar N, Soehartono AM, Chan KK, Zeng S, Xu G, Qu J, Coquet P, Yong K-T, Chen X. Nanocarbons for Biology and Medicine: Sensing, Imaging, and Drug Delivery. Chem Rev 2019;119:9559–656. https://doi.org/10.1021/acs.chemrev.9b00099.

[141] Patel KD, Singh RK, Kim H-W. Carbon-based nanomaterials as an emerging platform for theranostics. Mater Horiz 2019;6:434–69. https://doi.org/10.1039/C8MH00966J.

[142] Kong S, Zhang Q, Yang L, Huang Y, Liu M, Yan G, Zhao H, Wu M, Zhang X, Yang P, Cao W. Effective Enrichment Strategy Using Boronic Acid-Functionalized Mesoporous Graphene–Silica Composites for Intact N- and O-Linked Glycopeptide Analysis in Human Serum. Anal Chem 2021;93:6682–91. https://doi.org/10.1021/acs.analchem.0c05482.

[143] Ye X, Fan Q, Shang L, Ye F. Adsorptive carbon-based materials for biomedical applications. Eng Regen 2022;3:352–64. https://doi.org/10.1016/j.engreg.2022.08.001.

[144] Wang Y, Sun L, Guo J, Shi K, Shang L, Xiao J, Zhao Y. Pollens derived magnetic porous particles for adsorption of low-density lipoprotein from plasma. Bioact Mater 2021;6:1555–62. https://doi.org/10.1016/j.bioactmat.2020.11.015.

[145] Chen J, Ma Y, Wang L, Han W, Chai Y, Wang T, Li J, Ou L. Preparation of chitosan/SiO2-loaded graphene composite beads for efficient removal of bilirubin. Carbon N Y 2019;143:352–61. https://doi.org/10.1016/j.carbon.2018.11.045.

[146] Li Y, Li J, Shi Z, Wang Y, Song X, Wang L, Han M, Du H, He C, Zhao W, Su B, Zhao C. Anticoagulant chitosan-kappa-carrageenan composite hydrogel sorbent for simultaneous endotoxin and bacteria cleansing in septic blood. Carbohydr Polym 2020;243:116470. https://doi.org/10.1016/j.carbpol.2020.116470.

[147] Tyagi A, Ng YW, Tamtaji M, Abidi IH, Li J, Rehman F, Hossain MD, Cai Y, Liu Z, Galligan PR, Luo S, Zhang K, Luo Z. Elimination of Uremic Toxins by Functionalized Graphene-Based Composite Beads for Direct Hemoperfusion. ACS Appl Mater Interfaces 2021;13:5955–65. https://doi.org/10.1021/acsami.0c19536.

[148] Qiao L, Wang S, Du K. Macroporous cellulose/carbon nanotube microspheres prepared by surfactant micelle swelling strategy for rapid and high-capacity adsorption of bilirubin. Cellulose 2021;28:8419–28. https://doi.org/10.1007/s10570-021-04080-6.

[149] Song X, Xu T, Yang L, Li Y, Yang Y, Jin L, Zhang J, Zhong R, Sun S, Zhao W, Zhao C. Self-Anticoagulant Nanocomposite Spheres for the Removal of Bilirubin from Whole Blood: A Step toward a Wearable Artificial Liver. Biomacromolecules 2020;21:1762–75. https://doi.org/10.1021/acs.biomac.9b01686.

[150] Mikhalovsky SV, Sandeman SR, Howell CA, Phillips GJ, Nikolaev VG. Biomedical Applications of Carbon Adsorbents. Novel Carbon Adsorbents. Elsevier,; 2012. p. 639–69. https://doi.org/10.1016/B978-0-08-097744-7.00021-1.

[151] Zellner T, Prasa D, Färber E, Hoffmann-Walbeck P, Genser D, Eyer F. The Use of Activated Charcoal to Treat Intoxications. Dtsch Arztebl Int 2019. https://doi.org/10.3238/arztebl.2019.0311.

[152] WANG Z, CUI M, TANG L, LI W, WEI Y, ZHU Z, JIA X, KONG X, XU D. Oral activated charcoal suppresses hyperphosphataemia in haemodialysis patients. Nephrology 2012;17:616–20. https://doi.org/10.1111/j.1440-1797.2012.01626.x.

[153] Tominaga K, Sato S, Hayashi M. Activated charcoal as an effective treatment for bacterial vaginosis. Pers Med Universe 2012;1:54–7. https://doi.org/10.1016/j.pmu.2012.05.009.

[154] Dagar K, Pundir CS. An improved amperometric L-lactate biosensor based on covalent immobilization of microbial lactate oxidase onto carboxylated multiwalled carbon nanotubes/copper nanoparticles/polyaniline modified pencil graphite electrode. Enzym Micro Technol 2017;96:177–86. https://doi.org/10.1016/j.enzmictec.2016.10.014.

[155] Maiti D, Tong X, Mou X, Yang K. Carbon-Based Nanomaterials for Biomedical Applications: A Recent Study. Front Pharm 2019;9. https://doi.org/10.3389/fphar.2018.01401.

[156] Taqy S, Sarkar P, Hamid MA, Pranto T, Piner EL, Droopad R, Haque A. Diamond deposition on AlN using Q-carbon interlayer through overcoming the substrate limitations. Carbon N Y 2024;219:118809. https://doi.org/10.1016/j.carbon.2024.118809.

[157] Santra S, Bose A, Mitra K, Adalder A. Exploring two decades of graphene: The jack of all trades. Appl Mater Today 2024;36:102066. https://doi.org/10.1016/j.apmt.2024.102066.

[158] Wang Y, Weng GJ. Electrical Conductivity of Carbon Nanotube- and Graphene-Based Nanocomposites. Micromechanics and Nanomechanics of Composite Solids. Cham: Springer International Publishing,; 2018. p. 123–56. https://doi.org/10.1007/978-3-319-52794-9_4.

[159] Pirsaheb M, Mohammadi S, Salimi A. Current advances of carbon dots based biosensors for tumor marker detection, cancer cells analysis and bioimaging. TrAC Trends Anal Chem 2019;115:83–99. https://doi.org/10.1016/j.trac.2019.04.003.

[160] Arshad F, Nabi F, Iqbal S, Khan RH. Applications of graphene-based electrochemical and optical biosensors in early detection of cancer biomarkers. Colloids Surf B Biointerfaces 2022;212:112356. https://doi.org/10.1016/j.colsurfb.2022.112356.

[161] Williams RM, Lee C, Heller DA. A Fluorescent Carbon Nanotube Sensor Detects the Metastatic Prostate Cancer Biomarker uPA. ACS Sens 2018;3:1838–45. https://doi.org/10.1021/acssensors.8b00631.

[162] Kim E, Lee E-S, Lee D, Kim Y-P. Facile Determination of Sodium Ion and Osmolarity in Artificial Tears by Sequential DNAzymes. Sensors 2017;17:2840. https://doi.org/10.3390/s17122840.

[163] Fatoni A, Widanarto W, Anggraeni MD, Dwiasi DW. Glucose biosensor based on activated carbon – NiFe2O4 nanoparticles composite modified carbon paste electrode. Results Chem 2022;4:100433. https://doi.org/10.1016/j.rechem.2022.100433.

[164] Bortamuly R, Naresh V, Das MR, Kumar VK, Muduli S, Martha SK, Saikia P. Titania supported bio-derived activated carbon as an electrode material for high-performance supercapacitors. J Energy Storage 2021;42:103144. https://doi.org/10.1016/j.est.2021.103144.

[165] Freundlich HMF. Over the adsorption in solution. J Phys Chem 1906;57:1100–7.

[166] Hill TL. Theory of Physical Adsorption. Adv Catal 4 1952:211–58. https://doi.org/10.1016/S0360-0564(08)60615-X.

[167] Langmuir I. The constitution and fundamental properties of solids and liquids. Part II.-Liquids. J Frankl Inst 1917;184:721. https://doi.org/10.1016/s0016-0032(17)90088-2.

[168] A. Frumkin, Die Kapillarkurve der höheren Fettsäuren und die, (n.d.) 466–484.

[169] Huggins ML. Some properties of solutions of long-chain compounds. J Phys Chem 1942;46:151–8. https://doi.org/10.1021/j150415a018.

[170] Dubinin MM. The potential theory of adsorption of gasAL THEORY OF ADSORPTION OF GASES AND VAP. Chem Rev 1969;60:235–41.

[171] Anderson RB. Modifications of the Brunauer, Emmett and Teller Equation. J Am Chem Soc 1946;68:686–91. https://doi.org/10.1021/ja01208a049.

[172] Fritz W, Schluender EU. Simultaneous adsorption equilibria of organic solutes in dilute aqueous solutions on activated carbon. Chem Eng Sci 1974;29:1279–82. https://doi.org/10.1016/0009-2509(74)80128-4.

[173] Baudu M, Le Cloirec P, Martin G. Modélisations des isothermes d′adsorption sur charbon actif de composés aromatiques en solution aqueuse. Chem Eng J 1989;41:81–9. https://doi.org/10.1016/0300-9467(89)80075-9.

[174] Chen I. Great Barrier Reef: A Youngster to the Core. Sci N 1990;138:367. https://doi.org/10.2307/3974909.

[175] Cheng P, Hu YH. Dubinin-Astakhov model for acetylene adsorption on metal-organic frameworks. Appl Surf Sci 2016;377:349–54. https://doi.org/10.1016/j.apsusc.2016.03.124.

[176] Tóth J. Uniform interpretation of gas/solid adsorption. Adv Colloid Interface Sci 1995;55:1–239. https://doi.org/10.1016/0001-8686(94)00226-3.

[177] Zou L, Gong L, Xu P, Feng G, Liu H. Modified GAB model for correlating multilayer adsorption equilibrium data. Sep Purif Technol 2016;161:38–43. https://doi.org/10.1016/j.seppur.2016.01.026.